GEOCHEMISTRY AND ECOLOGY OF SALT PANS AT GUERRERO NEGRO, BAJA CALIFORNIA

FIELD TRIP No. 1 PREPARED FOR THE
GEOLOGICAL SOCIETY OF AMERICA
CORDILLERAN SECTION
1981 ANNUAL MEETING

MARCH 22-24

TRIP LEADERS:

W.T. HOLSER, DEPARTMENT OF GEOLOGY, UNIVERSITY OF OREGON, EUGENE OR 97403 U.S.A.

B. JAVOR, U.C.S.F., C.U.R.I.- 1315M SAN FRANCISCO CA 94124 U.S.A.

C. PIERRE, DEPARTMENT DE GEOLOGIE DYNAMIQUE UNIVERSITE PIERRE ET MARIE CURIE, 75230 PARIS CEDEX 05, FRANCE

ERRATA SHEET

Paper: "Geochemistry and ecology of salt pans at Guerrero Negro, Baja California", by W.T.Holser, B. Javor , C. Pierre and L. Ortlieb, in "Geology of Northwestern Mexico and Southern Arizona", L. Ortlieb and J. Roldán eds., 1981, p.1-56.

p.9, line 27, should read: "The corresponding seasonal variation in salinity of surface water in the inner lagoon is 42 to 51%, an increase....."

p.15, line 33, should read: "Huisache".

p.27, line 1, should read: "SABKHA".
line 26, should read: "rhombohedral".
line 26, should read: "(Pierre and Person, 1981)".
line 33, should read: "peaks".
line 37, should read: "rhombohedral".

p.30, Table 5, should read: "feldspar".

p.31, line 1, should read: "($7.20 < pH < 7.75$)".
line 19, should read: "(Pierre and Person, 1981)".
line 25, should read: "a calcium carbonate precursor".
line 30, should read: "HCO_3^-" .
line 39, should read: "SABKHA".

p.33, line 9, should read: "$CaCO_3$" .
line 21, the sentence: "(K^+) and (Mg^{2+}) ..... densities" should be placed after last sentence of p.39.

p.39, line 1, should read: "SABKHA".
line 27, should read: "centimetre".

p.46, the following references, at the beginning:

Alderman, A. R., and Von der Borche, C.C., 1961, Occurrence of magnesite- dolomite sediments in South Australia: Nature, v. 192, p. 861.

Barco, Miguel del, 1973, Historia natural y crónica de la antigua California (Annotated edition, by Miguel León-Portilla, of the manuscript of 1757): México, Instituto de Investigaciones Históricas, Universidad Nacional Autónoma de México, 404 p.

Bose, E., and Wittich, E., 1913, Informe acerca de la región occidental de la región norte de Baja California: Parergones del Instituto Geológico de México, v. 4.

Butler, G. P., 1970, Secondary anhydrite from a sabkha, northwest Gulf of California, Mexico: in Rau, J. L., and Dellwig, L. F. (eds.), Third Symposium on Salt, Cleveland, Northern Ohio Geological Society, v. 1, p. 153-155.

Calderon, F. I., 1924, La Concession Leese: Archivo Histórico y Diplomático Mexicano, p. 21.

Cardoso, J.N., Watts, C. D., Maxwell, J. R. Goodfellow, R., Eglinton, G., and Golubic, S., 1978, A biogeochemical study of the Abu Dhabi algal mats: A simplified ecosystem: Chemical Geology, v.23, p. 273-291.

Clavigero, F. J., 1937, The history of (lower) California (translated from the Italian edition of 1789 by S. E. Lake and A.A. Grayl): Stanford, California, Stanford University Press, 413 p.

p.47, line 15, should read: "Holser, 1979b".

p.54, line 10, should read: "island".
line 19, should read: "concentrators 1,2,3,4".

p.56, line 25, add, "Stop 14 is not shown in Fig. 27. It should be on the left of concentrator 2, about halfway between Stop 9 and the crossroad to Bahía Tortugas".

GEOCHEMISTRY AND ECOLOGY OF SALT PANS AT GUERRERO NEGRO B. C. S.

William T. Holser
Department of Geology
University of Oregon
Eugene, OR 97403, U.S.A.

Barbara J. Javor
U.C.S.F.
C.V.R.I. - 1315M
San Francisco, CA 94124, U.S.A.

Catherine Pierre
Dèpartment de Gèologie Dynamique
Université Pierre et Marie Curie
4 Place Jussieu
75230 Paris Cedex 05, France

Luc Ortlieb
Estación Regional de Noroeste
Instituto de Geología, U.N.A.M.
& Q.R.S.T.O.M., Ap. Postal 1159
Hermosillo, Sonora, México

ABSTRACT

Just south of Guerrero Negro, the 50 km length of Laguna Ojo de Liebre concentrates sea water to about 1.4X normal. Beyond the distal end of the lagoon, these waters flooded an extensive area of sabkha. An intertidal zone of dark algal mats includes precipitation of aragonite, high-magnesian calcite, and dolomite, and minor gypsum. The higher and more extensive part of the sabkha was reached only by occasional spring tides aided by storm winds which then precipitated gypsum and halite that was accumulated up to 2 m thick. Some brine remained interstitially to crystallize additional gypsum and halite, as well as polyhalite and magnesite (no anhydrite has been found).

In recent years most of the gypsum/salt flats have been covered by concentrating ponds for the production of salt. Mineralogy and geochemistry (major and minor elements and stable isotopes), of evaporite minerals and interstitial brines, are described for one section sampled prior to construction of the ponds, and for three taken from the periphery of the present ponds.

INTRODUCTION (W.T.H.)

Guerrero Negro is halfway down the Pacific coast of Baja California, 720 km south of the USA border on Highway 1 (Fig. 1). South of Guerrero Negro (GN), around the head of the Laguna Ojo de Liebre (LOL), was once the largest sabkha complex in North America (Fig. 2). Several smaller sabkhas occur elsewhere on both coasts of Baja California (Fig. 1). Beginning in 1957 the major part of the natural sabkha at LOL has been covered with ponds for solar concentration and crystallization, in turn making this the world's largest producer of salt. Both the remnants of the sabkha and the artificial ponds are unique laboratories for the study of the geochemistry and ecology of the hypersaline environment.

A few words concerning background of this trip and its leaders. In May, 1960, F. J. Phleger of Scripps Institution of Oceanography, who had studied the lagoons of the Mexican coast for many years (Phleger & Ewing, 1962), invited Holser to examine the unique evaporite deposits that were then still extensively exposed at LOL. Following this preliminary inspection, Holser returned to LOL in August, 1961, with J. R. Bradshaw of Scripps, for extensive sampling, including four shallow core holes. Holser returned again in May, 1965, with D. J. J. Kinsman for further surface sampling; subsequently they studied the 1961 cores. One result of this field work was a description of polyhalite replacing gypsum (Holser, 1966), largely from 1960 samples. Stable isotope data were published by Holser and Kaplan (1966), and Holser (1979b). Subsequently, Phleger (1969) and Kinsman (1969) published general descriptions of the LOL evaporites. Additional, previously unpublished data from the 1961 and 1965 samplings (which were in areas now covered by evaporating ponds) are given below. Holser's work at LOL was jointly supported by the Chevron Oil Field Research Company, and their contribution is gratefully acknowledged. In 1975 Holser, then in the Department of Geology at the University of Oregon, suggested to B. J. Javor of the Department of Biology that she might extend her previous work on algal ecology to higher salinities by studying those in the GN area. Javor spent several seasons in the field, and completed a Ph.D. dissertation (Javor, 1977, 1979). Subsequently she was employed as a biologist at GN by Exportadora de Sal, S.A., and is still continuing her biological studies at LOL.

In 1979 Ortlieb and Pierre began a geochemical and mineralogical study of the evaporites of Baja California, including three cross-sections at LOL outside the newer evaporating pans. These studies, including extensive chemical and stable isotope analyses of both sediments and brines, are continuing. One paper is in press (Pierre & Ortlieb, 1980), and that material as well as previously unpublished data is included in the description below, as well as in presentations at the meeting (Pierre, 1981; Pierre & Person, 1981). Ortlieb's investigations are part of a general study of the geodynamics of the Quaternary in the region of the Gulf of California, sponsored by Misión O. R. S. T. O. M. and by the Instituto de Geología, Universidad Nacional de Mexico. Pierre's investigations of stable isotopes are sponsored by the Comite national de recherche scientifique of France, and carried out in the Laboratoire d'hydrologie et de geochimie isotopique, Universite Paris-Sud, France.

In the following descriptions it was not always possible to integrate the earlier results of Holser with the more recent and intensive studies by

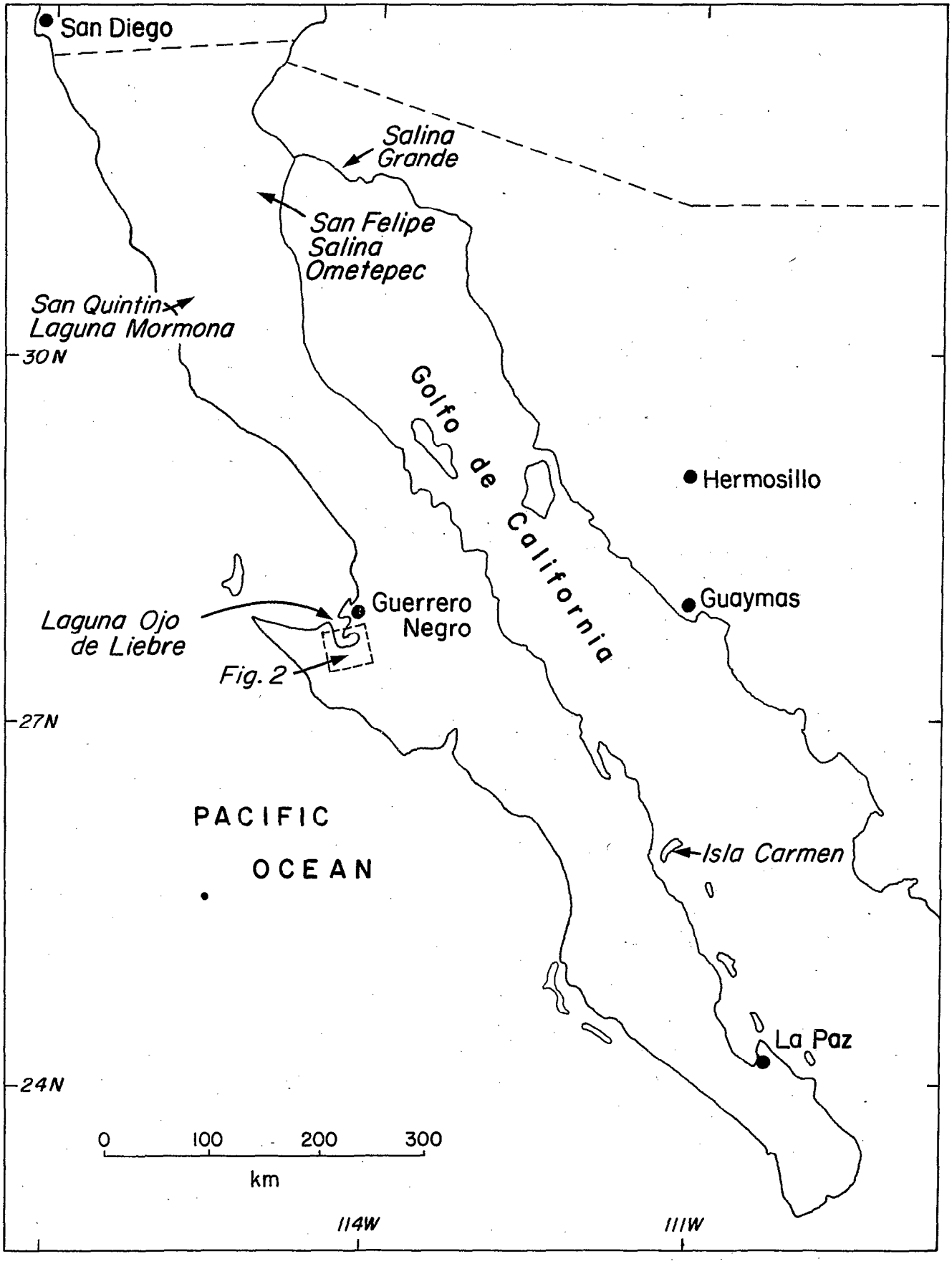

Figure 1. Index map of Baja California, locating Guerrero Negro and Laguna Ojo de Liebre, and other sabkha areas of Baja California.

Pierre and Ortlieb at LOL. Recent and continuing research at other sabkhas in Baja California (Fig. 1) is also relevant: Laguna Mormona (Vonder Haar, 1975; Horodyski & Vonder Haar, 1975; Vonder Haar & Gorsline, 1977; Pierre & Ortlieb, 1980), Laguna Ometepec (Kinsman, 1969; Butler, 1970; Shearman, 1970; Smith, 1973; Vonder Haar & Gorsline, 1977; Pierre & Ortlieb, 1980), and Salina Grande (Vonder Haar & Gorsline, 1977; Pierre & Ortlieb, unpublished).

HISTORY (W.T.H.)

The most dramatic era of this region's history began in November, 1858, when the whaler brig Boston, under Capt. C. M. Scammon, found a way through a narrow channel into the winter calving ground of the California Gray Whale (Scammon, 1868, 1969, 1970). Capt. Scammon named it Boston Lagoon, but it soon became famous as Scammon's Lagoon, a name that still competes with the older Spanish Laguna Ojo de Liebre. "Lagoon whaling" was extremely easy and profitable, although not without its dangers in smashed whaleboats, and the following winters saw a fleet of 10 or 20 whalers in the lagoon. By 1867, however, Scammon noted that " . . . so few whales are found there that it has been abandoned as a whaling ground; the decaying carcasses and bleaching bones strewed along the shores give evidence of the havoc made by the most enterprising and energetic class of seamen that sail under our national flag." Scammon went on to state that "The salt fields of Ojo Liebre are capable of supplying an almost unlimited quantity of excellent salt. . . . A year or two after the whaling commenced, vessels were dispatched from San Francisco, Upper California, for cargoes of salt; the first two, after cruising a length of time off the desired port, returned with the account that no such lagoon existed, or if it did, no channel could be found to get into it. A third vessel [brig Advance] was sent with a master determined to either find the place or 'break something'; he lost his vessel between Black Warrior [Guerrero Negro] and Upper Lagoon [Laguna Manuela]. Subsequently, the late Captain Collins, of San Francisco, a gentleman of much experience and a skillful seaman, obtaining the most reliable information at hand, sailed for the place that seemed to baffle the efforts of his predecessors to find. In due time, he arrived at the desired haven, without difficulty procured a cargo of salt, and returned to San Francisco. These voyages were followed up for a length of time, but the low price of the article compelled the proprietors to abandon the trade" (Scammon, 1868).

The salt of Laguna Ojo de Liebre was known to the Spanish missionaries before 1757; it was on the lands of Misión San Ignacio (Barco, 1973, p. 159; Clavigero, 1937, p. 31). However, the mission needs were apparently filled since 1717 by their salt works on Isla Carmen (Fig. 1) which lay only a few kilometers offshore in the Gulf of California. Calvigero's (1937, p. 30) description of that operation, published in 1789, is of both historical and geochemical interest.

"It begins at a distance of a mile and a half from the sea, and it extends for so many miles that the end is not seen with the eyes; it appears to the observer as an immense plain covered with snow. Its salt is very white, crystallized, and pure, without a mixture of earth, or of other foreign bodies. Although it is not so hard as rock salt, it is broken with picks, and in this manner it is cut into square cakes of a size such that each laborer can carry one of them on his back. This work is carried on in the first and the last hours of the day, because at other times the reflection

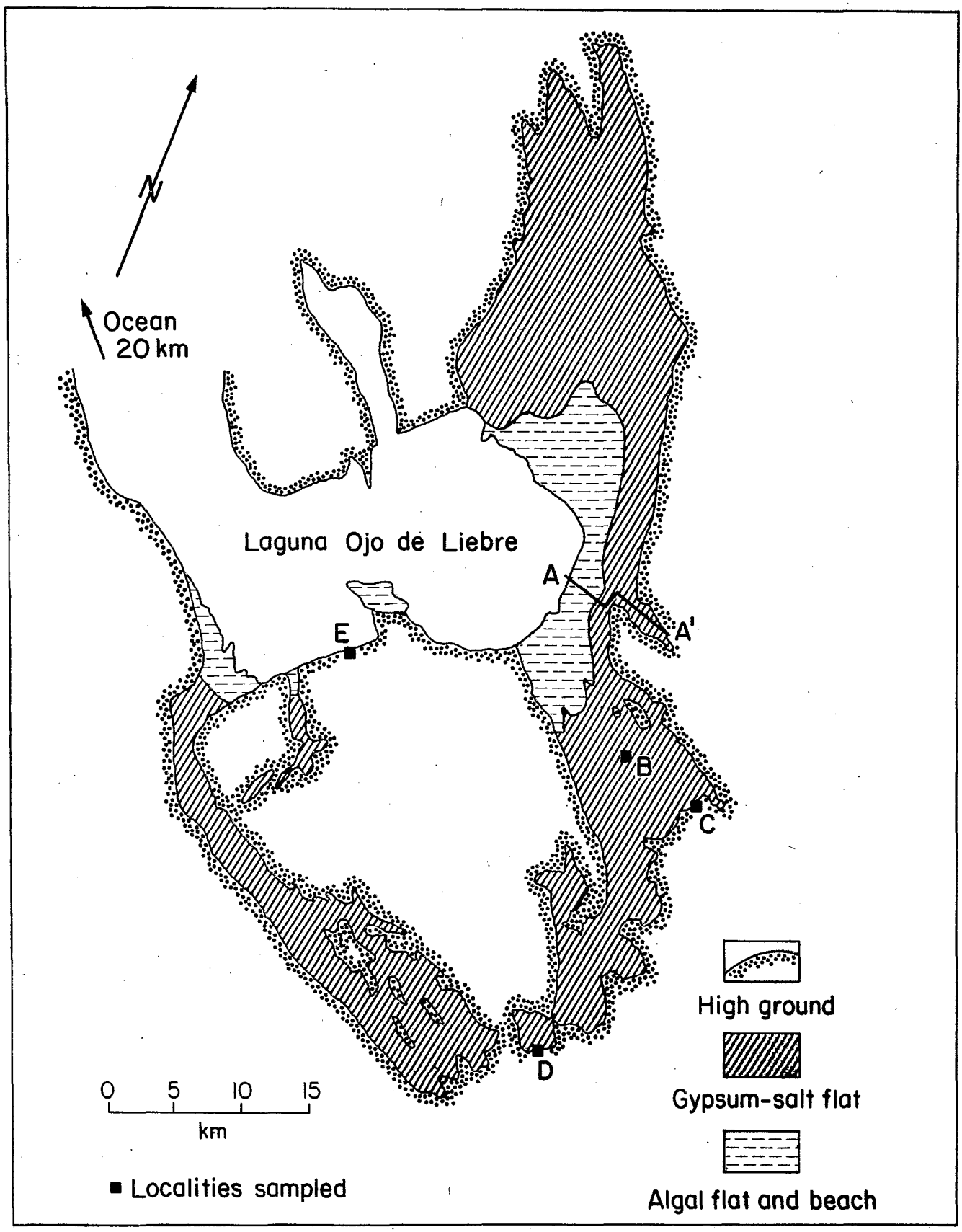

Figure 2. Map of the sabkha at Laguna Ojo de Liebre as it appeared prior to the construction of concentrating ponds, showing localities sampled both before (A, B) and after (C, D, E) pond construction, and reported in this guide.

of the rays of the sun on it is so bright that it dazzles the workmen. Although all the merchantmen of Europe might go there to load salt from the salt bed, they never could exhaust it, not only because of its great size but principally because all that salt which is taken from it is reproduced at once. When not more than seven or eight days have passed after the quantity necessary for loading a boat has been dug out, the excavation is rapidly refilled with new salt."

The Carmen Island salt deposit is a large pond nearly completely isolated by a Pleistocene coral reef, quite different from the situation at LOL: a modern description is given by Kirkland et al. (1966).

During the eighty years following the whaling period the salt of LOL was intermittently exploited. Due to the extreme isolation of this particular area, and the perennial disorganization of Federal control in this poor and distant territory of Mexico, the development could be carried on by clandestine operators. The Jefe Político of the Territorio de Baja California complained to the Agente de Fomento in Mexico City on 31 March, 1863, that Isla Carmen, Laguna Ojo de Liebre, and San Quintín were all being exploited, but were not under concession (Calderon, 1924). An expedition sent to Baja California in 1887 by the Secretaria de Fomento, found the remnants of a major industry, that had been precipitously abandoned by its operators. After being dug from the salt flats, the salt was moved by handcars on a track to the pier, where it was loaded onto 80-ton launches and transhipped in the lagoon to ships of 400 to 500 tons (Böse & Wittich, 1912-13, p. 408). The Chinese laborers were barely sheltered in small huts; a contemporary illustration vividly protrays the scene. Throughout this period occasional reference can be found to salt shipment into the port of San Francisco (e.g., Scammon, 1970), where it probably had to compete with salt won from the brines at Redondo and from the British operation at the Liverpool Salt Works on the playa at Salton, both much closer in southern California (Guinn, 1909).

In 1911-1912, a governmental expedition to explore the resources of Baja California thoroughly surveyed the salt deposits at LOL (and San Quintín). From logs of 45 test holes in the three salinas at LOL they estimated a resource of 14×10^6 T NaCl and described the deposits and their origin (Böse & Wittich, 1913, p. 343-409; Wittich, 1916).

Thus matters rested, more or less, until April, 1954, when Exportadora de Sal, S. A., began a modern operation of solar salt recovery. The present operations are described below. Under Daniel K. Ludwig of National Bulk Carriers they made their first shipment in 1957, with a production of 7×10^4 T, mainly to the west coast of the USA and Canada, and to Japan. In 1973, the company was sold to Mitsubishi Corporation of Japan, with the Mexican government retaining 25% of the stock. In 1976, the Mexican government, through the Commission of Mineral Development, acquired the majority of stock. Production is now 5.5×10^6 T per year.

In the meantime the California Gray Whale is back, the waters of the lagoon have been set aside as a nature preserve, and the area continues to fascinate both biologists and tourists with its unique display of the family life of the whale (Gardner, 1963).

PHYSIOGRAPHY AND GEOLOGY OF THE SABKHA AT LAGUNA OJO DE LIEBRE (W.T.H.)

The Laguna Ojo de Liebre extends 50 km into the Vizcaino Desert from the shore of Bahia Sebastian Viscaino and the Pacific Ocean (Fig. 1,2). The desert rises imperceptibly inland for another 50 km to the foothills of the Sierra de San Borjas. Sandy stream courses in this desert rarely carry runoff. Rainfall is sparse, over half of it falling in the winter months, and is highly variable from year to year (Hastings & Turner, 1965). The mean monthly maximum air temperature is 20-29°C, and the mean monthly minimum temperature is 8-20°C. West and west-northwest winds at speeds of 5 m/sec dominate the lagoon area over half the time. Although these are moist air masses off the Pacific, and dew is common at night or under an early morning overcast, evaporation is greater than precipitation by about 1.8 m/yr^{-1} (Phleger & Ewing, 1962).

Access of ocean waters to LOL is relatively limited: the single inlet between long sand bars is 4 km wide, and 9-12 m deep, with a vertical sectional area of about 0.04 km^2. An old (Pleistocene: Phleger, 1965) main channel up to 12 m deep extends to within 1-2 km of the sabkha, but much of the lagoon is shallow and some is exposed at low tide. The total area of evaporation in the lagoon complex is about 500 km^2, although all of this is not effective in concentrating the water at the distal end of the lagoon where it feeds the sabkha. The tidal range varies from about 1 to 3 m with turbulent velocities of 1.4 m/s at the entrance channel, slowing to 0.2 to 0.8 m/s in the distal part. In spite of this intensive tidal flushing, both the temperature and salinity of the surface water are strongly increased toward the distal area. As examples, a maximum temperature of nearly 25°C at the inner lagoon in June was 4°C warmer than surface water at the lagoon entrance. In February, the temperature of 19.5°C at the inner lagoon was 1.4°C warmer than at the entrance (Phleger & Ewing, 1962). The corresponding seasonal variation of surface water in the inner lagoon is 42 to 51°; an increase of up to 45% over the normal oceanic salinity at the lagoon entrance (Phleger & Ewing, 1962; Holser, unpublished).* Thus warm, dense brines are being formed at the inner lagoon surface, which feed the sabkha and also apparently intermittently reflux to the ocean. "At most times the water (in vertical section in the lagoon) is isohaline with depth at all stations. At a few stations the bottom salinity was significantly higher than that at the surface. This was most pronounced on the morning of July 19, 1956, when salinity in the inner lagoon at the surface was 46.7°/oo and at the bottom 47.8°/oo, in the channel (halfway to the entrance) at the surface 28.3°/oo and at the bottom 38.3°/oo, and in the lower lagoon main channel at the surface 35.8°/oo and at the bottom 36.8°/oo. These data suggest that somewhat more saline and therefore more dense bottom water was being formed in the inner lagoon on [that date] and was flowing seaward along the bottom of the channel. . . . It is conjectured that, in a lagoon, the phenomenon operates on a diurnal rather than a seasonal cycle as in the more open seas [such as the Mediterranean and the inner Gulf of California]. Data are insufficient to allow generalization

---

*No data are given by Phleger to support his later estimate (Phleger, 1969, p. 825) of ". . . a salinity almost twice that of the adjacent open ocean."

on the frequency or magnitude of this mechanism in Laguna Ojo de Liebre. Limited observations suggest that it is infrequent, but observations were not made at night when such a process is expected to be most active" (Phleger & Ewing, 1962, p. 827). The tidal conditions for the above salinity observations were not stated. In another publication, Phleger (1969, p. 827) states, in contradiction to the above specific data "No evidence was discovered of a possible return flow of saline water out of the lagoon . . ."

The border between the upper lagoon and the sabkha (Fig. 2) is marked by a low beach ridge of sand, composed mainly of quartz, plagioclase, and hornblende, with varying amounts of carbonate shell fragments and oolites. Sands elsewhere in the lagoon contain pelletal apatite (Phleger & Ewing, 1962), but none was found at this beach. The beach ridge is breached by a number of tidal creeks, which are bordered by a carpet of Salicornia and Spartina that makes them show as black winding patches in Figure 3.

Many daily tides and especially semi-monthly spring tides flood an area behind the beach ridge, dominated by black, rubbery mats of blue-green algae which show as gray areas in the aerial photograph of Figure 3. The algal mats originally covered an area of about 100 km^2 (Fig. 2). The mats include interstitial aragonite, high-magnesian calcite (HMC), dolomite, and gypsum, as will be described in detail below.

Beyond the algal mat area the flats were covered with a hard crust of gypsum and halite, showing as brilliant white in Figure 3. These salt flats originally extended about 500 km^2. The lagoon side of this area was flooded by many tides, with evaporation sufficient to produce a visible floating film of gypsum and halite crystals. The shoreward parts of the salt flats were beyond the reach of normal tides, but apparently storm surges and persistent onshore winds were able to drive a layer of lagoonal water to the farthest reaches of the flats (Phleger, 1969). This intermittent inflow, probably one or more times a year, was documented by swash marks composed of shells, seaweed and other flotsam that wound across the flats. This kind of storm flooding was documented for Laguna Mormona, Laguna Ometepec, and Salina Grande (Fig. 1) by satellite photographs (Vonder Haar & Gorsline, 1975). The resulting deposit of salt and gypsum varies from a few millimeters thick at its lagoonward edge, to a maximum of 2.5 m. The wide-ranging survey of Böse and Wittich (1916, p. 388-398) showed salt/gypsum thicknesses generally in the range of 10 to 20 cm.* The mineralogy of the evaporite deposit includes gypsum of various morphologies; halite, polyhalite, celestite, magnesite and bassanite, as described below in detail for sections A, C, and D. The evaporite displays a succession of irregular layers 0.2-2 cm thick of light evaporite minerals alternating with darker layers of organic debris and windblown sand.

The porosity of the salts and underlying sands is permeated by a bittern brine. According to Phleger (1962) the brine is residual to evaporation of the surface flooding described above, and "The brine and

---

*Although Böse and Wittich (1913, p. 386) state that, "La localization de estos pozos está marcada en el bosquejo de carte que acompaña a este informe . . .," no such map of their sampling locations seems to have been published.

evaporite areas seem to be essentially a closed system retaining all the salts present in seawater. No return of brines to the lagoon could be detected, although a minor amount of seepage may occur." It is not clear what tests Phleger could have made would have precluded reflux of the brines to the lagoon. On the land side of the sabkha, although no surface runoff is apparent in the present regime, ground water in wells is fresh, both at the town of Guerrero Negro and at Ojo de Liebre ("Rabbit Well," from which the lagoon derives its name). The relation of such continental subsurface waters to the sabkha brines is unknown.

During all the early work it was clearly recognized that the hydrologic regime could only be demonstrated by a precise levelling of the water table, coupled with a tide gauge at the beach, but such measurements were never made and it is now too late to make them.

The evaporite section is underlain by sands and silts, with isolated crystals of gypsum, halite, and occasional small aggregates of polyhalite, probably crystallized in place. The "high ground" (Fig. 2) surrounding the salt flats and inaccessible to the highest storm tides, is similar in nature to that underlying the salt. In various places, old semi-consolidated alluvium, beach rock and both new and old gypsum dunes may be recognized.

The morphological origin of the depressions occupied by the sabkha salt and gypsum is obscure. According to Phleger (1969) the oldest parts of the sabkha deposit are more than 30,000 years old including one or more Pleistocene interglacials (Phleger, 1969). On the other hand, Phleger (1965) dates the offshore bars that originally enclosed these lagoons (and which must therefore have preceeded the sabkha of the inner lagoon) as accompanying the post-Pleistocene rise of sea level about 6,000-7,000 years B.P. Mina (1957) lists 48 m of Pleistocene quartz sands and 150 m of Pliocene-Miocene sands and clays at the top of the section in the well San Francisquito no. 1 nearby at Lagunitas. According to Phleger (1969) "Abundant evaporites have been found to a depth of 200 m in the cuttings from a water well near the northern edge of the Ojo de Liebre halite flats. These subsurface evaporites may be deposited by interstitial circulation of brine and precipitation of salt within the sediment. They also may represent older deposits that were precipitated when relative sea level was lower than it is today." It is clear that much remains to be learned concerning the geological and paleogeographical setting of these sabkha deposits.

One aspect of sabkha history seems clear: if the concentration of inflowing brines is sufficient to precipitate halite, as it is at LOL, the level of the sabkha always remains uniformly at a little above any relative rise of sea level. This is true not only on a geological but even on an historical scale. The old descriptions cited above of the Carmen Island deposit, and experience elsewhere, indicates that substantial excavations will be "healed" by new salt within a year. Of the undetermined but undoubtedly large tonnage of salt that was dug out of the LOL salt flats in the century from 1860 to 1960, no sign of excavation remains, even on aerial photographs. This fact also leaves some ambiguity in the interpretation of these deposits as natural geological features, including the results of drilling described below.

The mineralogy and geochemistry of the minerals and brines will be described for four separate sections of the sabkha. It is not yet possible to present an integrated picture of the geochemistry, and research is continuing by Pierre and Ortlieb.

BIOLOGY AND BIOCHEMISTRY OF THE SABKHAS (B.J.J.)

General Discussion

Temperate salt marshes around the world tend to have similar biological community structures (Larsen, 1980). Among the higher plants, the lower intertidal is dominated by the grass Spartina while the upper intertidal is dominated by a Salicornia (pickleweed) assemblage. Blue-green algae are a nearly ubiquitous part of the flora of salt marshes and intertidal shores around the world. In some places, their presence may be detected only through enrichment cultures. In other environments, color-banded beach sand ("Farbstreifensandwatt") composed of vertically zoned communities of eukaryotic algae, blue-green algae, colorless sulfur bacteria, and purple sulfur bacteria develop in loose, intertidal sediments under protected conditions. In still other environments, blue-green algae form thin to thick peats which may or may not calcify. In spite of their cosmopolitan distribution, blue-green algal communities fail to develop into stromatolites in most modern intertidal environments.

The upper intertidal limit of blue-green algal distribution is apparently related to limits of dessication. The lower limits to algal mat distribution have been attributed to current velocities, grazing pressure, and competition from higher algae and plants. Little is known about why eukaryotic algae generally do not inhabit stromatolite environments. In some mats, eukaryotic and prokaryotic algae coexist.

Intramat and submat reducing conditions, and the presence of H_2S in marine mats are common. Often a rich photosynthetic bacterial flora develops as a one-to-several-mm-thick pink lamination directly below the top layer of blue-green algae.

Preservation of the organic component of laminated algal sediments is promoted by anaerobic conditions beneath the mat surfaces. It has also been suggested that low oxidation potentials in the water may inhibit decomposition. When anaerobic conditions remain undisturbed in some Persian Gulf sediments the cellular structures have been preserved as long as 8000 years.

Most environments where $CaCO_3$ precipitation is occurring within modern marine stromatolites are moderately to highly hypersaline. The carbonate system in moderately hypersaline seawater is virtually unstudied. Predictions of solution and precipitation processes of $CaCO_3$ must be based on knowledge of activity coefficients, solubility products, and ionic interactions that are empirically derived. In these particulars the geochemistry of environments inhabited by stromatolites, and the geochemistry of their morphogenesis, are very poorly understood.

Algal Communities at Lagunas Guerrero Negro and Ojo de Liebre

Intertidal algal mats develop in some of the slightly hypersaline marshes and in many of the moderately hypersaline flats. General geological and climatological aspects, as well as the general biology of the blue-green algal communities of these lagoons, are very similar to those environments described on the Abu Dhabi coast of the Persian Gulf (Cardoso et al., 1978), the Laguna Madre area of the Texas Gulf coast, and the Laguna Mormona area of Baja California (Fig. 1; Horodyski & Vonder Haar, 1975).

The major mat types each correspond to the lower, middle and upper intertidal. In the lower intertidal mat, the top photosynthetic layer is actually a bilayer composed of a surface blue-green algal horizon dominated by Microcoleus chthonoplastes (about 3 mm thick), and an underlying purple layer of photosynthetic bacteria predominantly Chromatium sp. (about 2 mm thick). The mat may accrete to a thickness of 10 cm or greater, and is characterized by fine laminations of alternating blue-green algal and photosynthetic bacterial layers. The middle intertidal is characterized by a relatively thin (up to several cm) mat dominated by Lyngbya aestuarii, and only a thin, lower horizon of purple photosynthetic bacteria. One-cm-tall pinnacles that resemble the Precambrian stromatolite, "Conophyton," occur locally in the Lyngbya mats. The upper intertidal is characterized by a crusty, wrinkled mat dominated by Calothrix crustacea. Total mat thickness is about 0.5 cm. None of the mats is lithified.

Experiments on the photosynthetic potential of algal mats in the field gave the following results: temperature optima between approximately 35 and 40C; all mats were inhibited photosynthetically under full sunlight and they demonstrated maximal photosynthetic rates at about 300-600 W/m^2 (full mid-day sunlight is about 1000-1200 W/m^2); salinity optima relative to normal seawater were Microcoleus mat = 0.4-1.5X, Lyngbya mat = 1.2X, and Calothrix mat = 1.5X; and none of the mats was apparently inhibited by high concentrations of O_2.

Two grazing invertebrates, a gastropod (Cerithidea californica) and a waterboatman (insect: Trichocorixa sp.), are dominant biological factors that limit mat distribution. The mats in effect find refuge from the very destructive cerithids by their ability to grow in environments that exclude the gastropods. Cerithid populations are promoted by: proximity to a fresh source of seawater, and soft and moist subaerial sediments. Waterboatmen are nearly ubiquitous in these environments but they never completely decimate mats. They are restricted by elevated salinities and short lifetimes as adults. Because the Microcoleus mat is the fastest growing, and because many of the sediments are bare in the lower intertidal range of the lagoon, invertebrate grazers apparently restrict Microcoleus mat development on all lower intertidal sediments except those in isolated pools.

Aragonite precipitation occurs in the mats. In Laguna Guerrero Negro, non-mat sediments are silicoclastic sands, so the precipitation of $CaCO_3$ in the mats could be measured. Absolute $CaCO_3$ content increased with total mat thickness and organic carbon content. $CaCO_3$ content decreased with depth in the mats, demonstrating that in a predominantly silicoclastic, slightly hypersaline environment, the $CaCO_3$ produced in the mats is not stable. Organic geochemistry of the mats has been described recently by Philp et al. (1978).

Bacteria in the Concentrating Ponds

It is well known among solar salt company managers that the pink coloration of brines increases the solar absorption of the brines (heat) and thus enhances evaporation and precipitation. Temperatures of colored brines are almost invariably higher than those of clear brines in the same saltern at any particular time of day. The cause of the coloration is the great proliferation of brine bacteria (halobacteria).

Under conditions of increasing brine concentration of marine seawater, such as is found in commercial salterns, is there an upper brine concentration that limits halobacterial distribution? In the E.S.S.A. saltern, pigmented bacteria are not found in the bitterns. Brines are very pink until a density of about 1.26 and they are brownish grey at a density of 1.27. At higher densities, brines are green, either clear or opaque (due to suspended salt crystals), which apparently is the natural color of the brines without pigmented bacteria. Brines up through the bitterns stage were recently plated and are now being identified. It is unknown at this time whether viable bacteria that might be found in the bitterns are reproducing in that environment.

SALT PRODUCTION AT GUERRERO NEGRO (E.S.S.A.)

Common salt, or sodium chloride, is a very abundant mineral, and is widely used in the chemical and food industries as well as for de-icing roads. Exportadora de Sal, S.A., operates the largest solar salina in the world, and exports all of its production of about 5.5 million tons per year to Japan, the United States and Canada.

The concession authorized to the company by the Mexican government is 39,995 hectares. This consists of two main areas: 21,500 hectares for concentration subdivided into 13 areas in order to control the evaporation process; and 3700 hectares for recrystallization subdivided into 49 areas, named vasos. These ponds are divided by means of 175 km of dikes, of which 111 km in the concentration area is protected to prevent erosion by wind and wave action. Within the system there are another 30 km of canals and 30 km of major transport roads.

There is also a salt washing plant and port facilities for loading barges in an area called Chaparrito. In Guerrero Negro there are shop facilities for maintenance, administrative offices, houses for company personnel, a hospital, church, primary and secondary schools, and recreational facilities. The population of Guerrero Negro is 5400, of which 580 work for E.S.S.A.

Drinking water is taken from six wells, approximately 20 meters deep, and pumped to town and company facilities by means of 10 km of pipelines. Energy is provided by a generator of 1500 kW, two of 730 kW, and two of 800 kW. There are 20 km of transmission lines for the distribution of electricity.

The seawater of Laguna Ojo de Liebre, with a density of 1.0313 and NaCl content of 3.5%, is pumped into the first concentration area by 10 pumps of 1.06 meters in diameter, with a total capacity of 1190 m^3/min. This water passes through the concentrating area, and by means of solar evaporation becomes saturated with NaCl. It is transferred to the crystallization area at a density of 1.221 and 22.5% NaCl.

In the crystallization area, the brine deposits 80% of its contained salt. Upon reaching a density of 1.255, the brine is pumped out. This is why the company is developing studies for the recovery of by-products from these bitterns.

Every crystallizing vaso is harvested twice a year. The thickness of the layer of harvested salt is approximately 12 cm. The vasos are first completely drained by pumps, scraped and piled in rows by snowplow-like machines, then collected by harvesters. The salt is lifted in the

harvester by means of an elevator belt consisting of salt scoops and a rubber belt. The harvesters were specially designed for the company. Each one has a capacity of 2000 tons per hour.

The salt is transported about 12 km to the washing plant by means of five Kenworth Dart trucks, each one with three trailers. The capacity of each trailer is 120 tons.

The Kenworth Dart trucks unload the salt in the hopper at the washing plant. The hopper feeds eight stainless steel belts where the salt is first rinsed with brine of density 1.174, and then with seawater. This removes and dissolves the superficial impurities from the crystals (insoluble material and salts of calcium and magnesium), increasing the purity from 98.5 to 99.5% NaCl.

After washing, the salt is sent by conveyor belt to a stockpile with capacity of 100,000 tons. Alternatively, it is directly loaded onto barges by means of a system of conveyor belts with a capacity of 1800 tons per hour.

The salt is transported 100 km (moved by five tug boats with a power of 2500 to 3500 H.P.) from Guerrero Negro to Cedros Island. Cedros Island has three unloading docks with a capacity of 1800 tons per hour. The barges are self-unloading, having a conveyor belt below. The capacity of the stockpile of salt on Cedros Island is 900,000 tons.

The dock in Cedros Island has a length of 221 meters and a depth at low tide of 18 meters. It can load ships up to 156,000 tons capacity. The salt is taken from the stockpile at Cedros by means of a machine made by Barber Green, which has a capacity of up to 3000 tons per hour. The system for loading ships consists of conveyor belts and a telescopic hopper.

MINERALOGY AND GEOCHEMISTRY OF SABKHA SEDIMENTS AND BRINES: SECTION A (W.T.H.)

Sedimentary Deposits

Section A (Fig.s 2, 3, 4) extends from the distal shore of LOL at the abandoned salt-loading tramway known as the "English Bridge" in a nearly easterly direction across the algal flats, then jogs to the north before continuing up the center of a prominent embayment in the salt flat ("Salina Chica" of Böse and Wittich, 1913; currently called "Huizache"). Before construction of the concentrating ponds this section was the most accessible, and was sampled several times. In the central part of this section four holes were cored and sampled down to bedrock (Fig. 5).

Beyond a low beach ridge of detrital sand, black mats of algae cover the first 2 km of the section, and control the carbonate mineralogy that is mixed with the clastic sands. As evaporative concentration increases eastward, evaporite minerals begin to accumulate, although with a continuing component of clastic material as well as layers of decomposing salt grass and other organic flotsam (Figs. 6, 7). In the embayment evaporite minerals clearly dominate the upper layers. The drilled sections (Fig. 5) show several meters of sands and silts underlying the whole sabkha with variable amounts of dispersed diagenetic evaporite minerals.

Although lines in Figure 5 suggest some correlation of sedimentary beds, these are probably not very significant--the changes of sediment type are rather discontinuous, as are the individual mm-to cm-layers that are evident in much of the sediment (Figs. 6, 7).

Figure 3. Aerial view of a cross section (A in Fig. 2) of the sabkha before construction of concentrating ponds. The distal end of the lagoon, and the beach, are in the foreground, followed by the gray intertidal algal flats cut by black tidal creeks. Gypsum-salt flats are stark white, reaching their greatest thickness and degree of concentration in the embayments beyond. The sampled section A follows the causeway of the "English Bridge," which is seen as a straight line leading from the lagoon in the lower right. Reproduced from Holser (1966), with permission of The American Mineralogist.

Mineralogy

Qualitative X-ray diffraction, microscopy, and field observations (by D. J. J. Kinsman and W. T. Holser) show an interesting pattern of mineralogy, as laid out in Table 1.

Sediments under the algal mats include much carbonate mud. High-magnesian calcite (HMC) of 2-3 mm size dominates; X-ray determinations (± 1-2 mole percent $MgCO_3$, using an Si standard) show from 10 to 14 mole percent $MgCO_3$. The HMC is consistently associated with debris of Zostera encrusted with foraminifera and red algae. Dolomite is also common, presumably replacing HMC: it contains 44-47 percent $MgCO_3$ and all of it shows some degree of ordering.

During the 1965 field work D. J. J. Kinsman discovered magnesite at LOL, which he briefly reported previously (Kinsman, 1969), and the following description is supplied by him (personal communication, 1966). It was found (sample 24822-1) in the salt flats (Fig. 4) in a porous layer of quartz-feldspar sand, at 7 cm depth, as 3-mm, hard, dead-white blebs, associated with 3-mm discoidal gypsum crystals and rare celestite needles. The magnesite aggregates were composed of 1.5-μm equant grains. X-ray diffraction confirmed magnesite, with a = 4.658, c = 15.134A, compared to a standard (XRPDF starred pattern 8-479) a = 4.6332, c = 15.015A. The expanded lattice could be accounted for by a substitution of 7 mole percent $CaCO_3$, and this is confirmed by atomic absorption analysis of a carefully cleaned sample: Ca^{2+} 36,150 ± 250 ppm, Sr^{2+} 2.8 ± 1.1 ppm. An expanded lattice is characteristic of Recent magnesites including those of the Trucial Coast on the Persian Gulf (Kinsman), South Australia (Alderman & Von der Borche, 1961), and Great Salt Lake (Graf et al., 1961), although in the latter case the total foreign cations failed to account to the expanded lattice. The HMC and dolomite found in the algal mat area are absent in the salt flats--and even magnesite is only sporadically present there. Huntite, $Mg_3Ca(CO_3)_4$, previously found in the Trucial Coast sabkha (Kinsman, 1967), was looked for but not found at LOL.

Gypsum is ubiquitous at LOL, most evident as layers of coarse crystal mush (Fig. 6, 7), but also common as aggregates and as larger poikilitic crystals in the underlying sands. A discoidal morphology is common, but in fact, a wide variety of growth forms and features are found at LOL and these have not been systematically studied.

Six gypsum samples from core holes on the salt flat (Figs. 4, 5) were analyzed by optical emission spectrography by R. E. Wolven of Chevron Oil Field Research Company. Sr contents were 18136-2 3600, 18136-5 5800, 18136-9 1600, 18136-14 250, 18136-18 380, and 18137-12 1700 ppm. The first two samples are aggregates, in which the presence of celestite cannot be precluded. The purest single gypsum crystals are 18136-9 and 18137-12 (as verified by SiO_2 levels of 0.07 and <0.04 percent), and their strontium levels are consistent with those reported by Butler (1973) in his detailed study of strontium in the Trucial Coast. Other trace elements in these two pure samples are B <3, <3; Ba 3.5, 5; Fe <30, <30; Mg 400, <100; and Mn <3, <3 ppm. It may be significant that the two other samples from hole 18136, which occur as 1- to 2-cm crystals poikilitically enclosed sand grains in sands several meters below the evaporite layers, are an order of magnitude depleted in Sr.

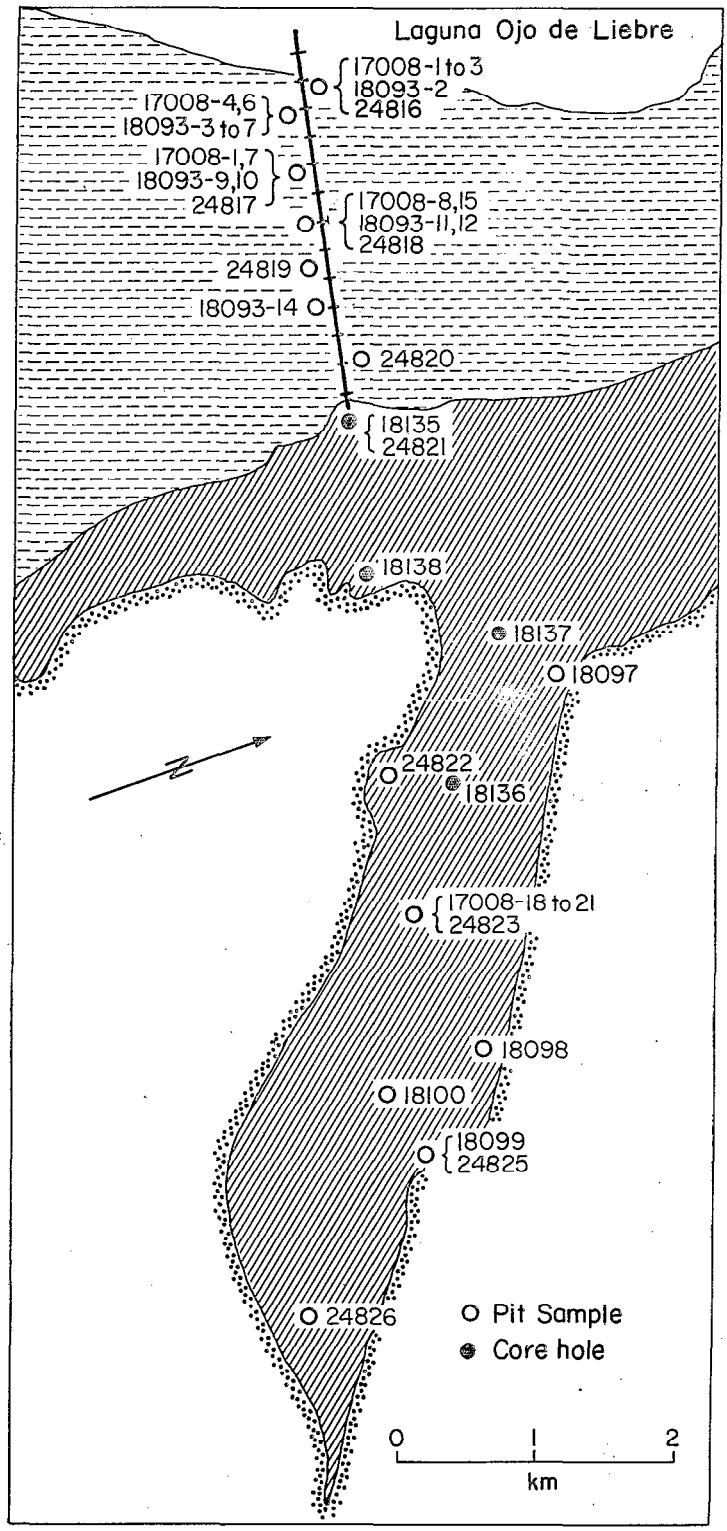

Figure 4. Map of Section A of Figure 2, showing sampling of May, 1960 (17008), August, 1961 (18093-18138), and May, 1965 (24815-24827), all prior to pond construction in this area.

Table 1. Qualitative Mineralogy of Near-Surface Sediments Along Section A, west (lagoon beach) to east (high ground) (Figs. 2-5)

	24816	18093-3	24817	24818	18093-14	24820	See Fig. 5: 18135	18138	18137	18136	18097	24822	24823	18098	18100	24825	24826
Quartz	D	D	M	T	T	T	M	–	–	T	T	D	–	–	–	D	D
Plagioclase	M	T	–	T	M	–	–	–	M	T	–	D	–	–	–	D	D
Mg-calcite	D	D	D	D	M	M	T	–	T	T	–	–	–	–	–	–	–
Dolomite	M	–	–	M	–	–	M	–	T	–	–	–	–	–	–	–	–
Gypsum	T	M	M	M	M	M	D	D	D	D	D	D	–	–	M	M	–
Halite	–	–	T	T	T	T	T	T	D	D	D	D	D	D	D	D	D
Polyhalite	–	–	–	–	–	–	–	–	–	M	–	–	M	M	M	M	D
Magnesite	–	–	–	–	–	–	–	–	–	–	–	D	–	–	–	–	T
Celestite	–	–	–	–	–	–	–	–	–	–	–	M	–	–	–	M	–

X-ray diffraction analyses by D. J. J. Kinsman and W. T. Holser, supplemented by field observations.
D = dominant; M = moderate; T = trace; – = not observed (absent, or in some cases not looked for).

At one locality (24825, Fig. 4) a euhedral crystal of gypsum enclosed a core of white bassanite, $CaSO_4 \cdot 1/2H_2O$. Surprisingly, a thorough search both in the field, and in laboratory examination of samples, failed to detect any trace of anhydrite at LOL. Celestite was detected in two samples on the salt flat (Table 1) as 10-μm-long needles; probably it is more widely distributed but unrecognized.

Halite is ubiquitous in the salt flat area. It can be observed crystallizing with gypsum in sheets of tidal water one to a few centimeters deep, both as a floating film of crystals and as a crust on the bottom. Larger crystals, up to 2 cm, occur both in the layered evaporite body and sporadically in the underlying sands. Cube morphology is common, but the incidence of hopper crystals, chevron growths, and other morphological variations has not been systematically studied at LOL. Deposition of gypsum and halite grossly overlap, with no clear horizontal or vertical zonation.

Bromide is an important trace element in halite (for a survey of bromide geochemistry of salt rocks see, for example, Holser, 1979b). Table 2 lists some bromide analyses of salts from Section A—the multiple values are separate analyses of subsamples, mostly distinct crystals of halite from the same general part of the core. Values in the expected range of primary initial crystallization from a marine brine are found both at the western end of the salt flat, and far into the salt flat. But in the thickest salt (hole 18136) the values are about twice, mean 156 ppm Br/NaCl at all levels in the core, with a moderate variation of $2\sigma = \pm 46$ ppm. This indicates that the brines from which these salts crystallized were concentrated in the range 20-40X sea water. This concentration agrees with the analyses of the brine presently permeating the salt flat, as shown below (Table 3).

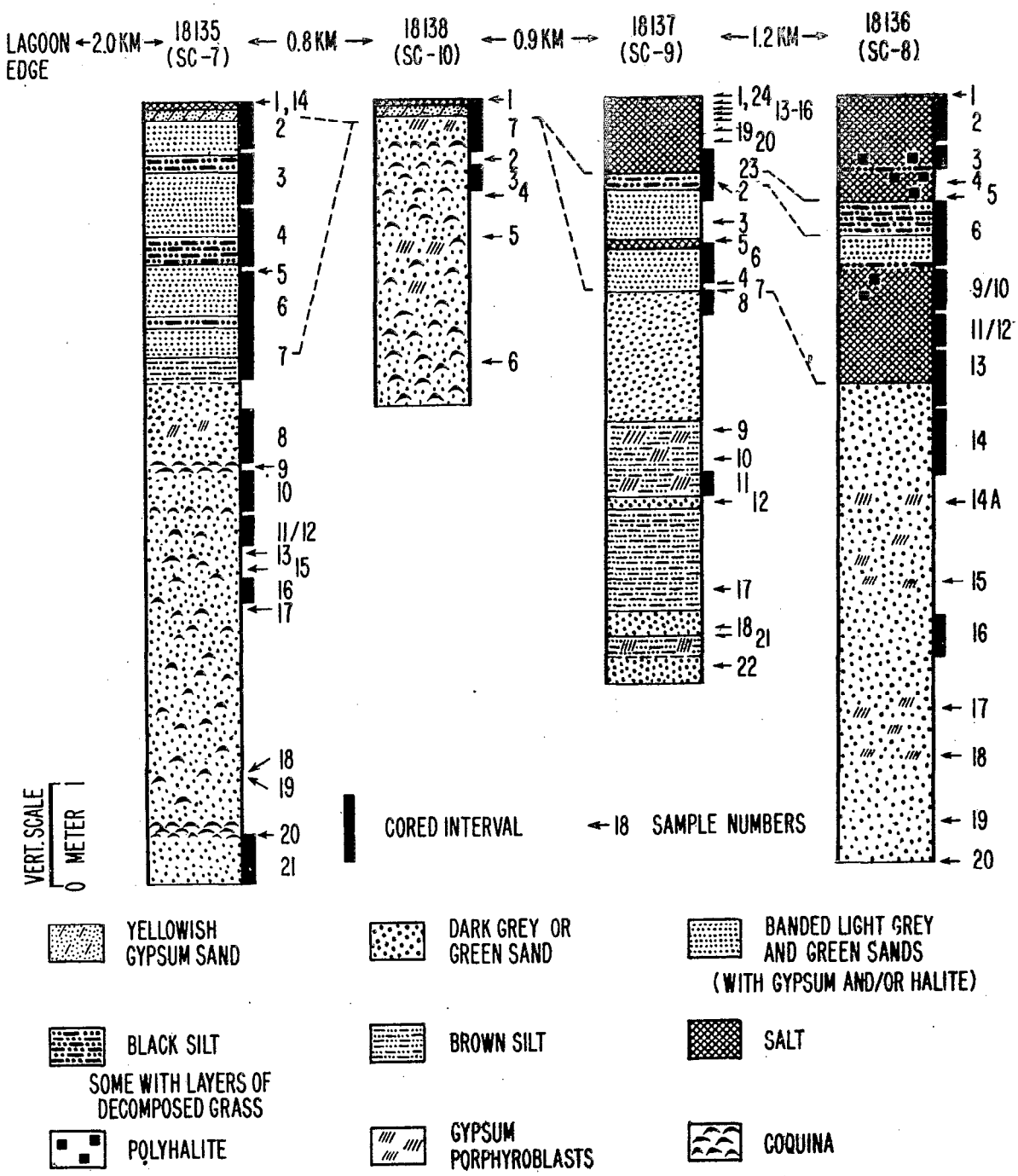

Figure 5. Field logs of the four core holes in the mid-part of Section A (Fig. 4).

Table 2. Bromide Analyses of Halite Along Section A

Sample no.[a]	Br/NaCl, ppm[b]
17008-9	67
18137-13	72
-16	94
18136-2	121, 153, 122, 179, 171
-3	195, 137, 186 123, 100
-4	129
-5	120
-9	168
-11	106, 149, 269
-13	208
-16	82, 123, 157, 68
17008-18	92
-19	51

[b]Analyses by Gale Baker, Chevron Oil Field Research Co., chloramine-T method.
[a]For positions of samples see Figures 3, 5.

But it is still not clear, as indicated earlier (Holser, 1966) on the basis of very limited bromide data, why halites on the more distal salt flat (17008-18, 19), where even polyhalite is precipitated, have again the lower levels of bromide.

Polyhalite ($K_2MgCa_2(SO_4)_4 \cdot 2H_2O$) at LOL was the first discovery of the mineral in Recent sediments, and its occurrence was detailed in a previous publication (Holser, 1966). Curiously, since that description, it does not seem to have been confirmed from other Recent sabkhas. It was found at many places in the central and distal parts of the salt flats (Table 1), in sections A (Fig. 3), B (Fig. 2) and C (Fig. 2; see below). It occurs as a dead-white caliche-like mass just under the water table (Fig. 6), as well as dispersed aggregates in the underlying sands (Fig. 5). Much of the polyhalite replaces previous gypsum euhedra as a mass of 5-μm fibers, in many cases roughly oriented perpendicular to the crystal face of the gypsum (Fig. 8). Some polyhalite also appears to be in an interstitial precipitate, but the presence of a fine-grained gypsum precursor cannot be excluded. In most, but not all, polyhalite samples some remaining gypsum is still apparent. Polyhalite from other sections of the sabkha is described by Pierre (1981), and in this guide.

Brines Chemistry

Chemical analyses of a sequence of brine samples are shown in Table 3, arranged geographically from the lagoon on the left, across the algal flats, and through the salt flats. This chemical data should be considered as

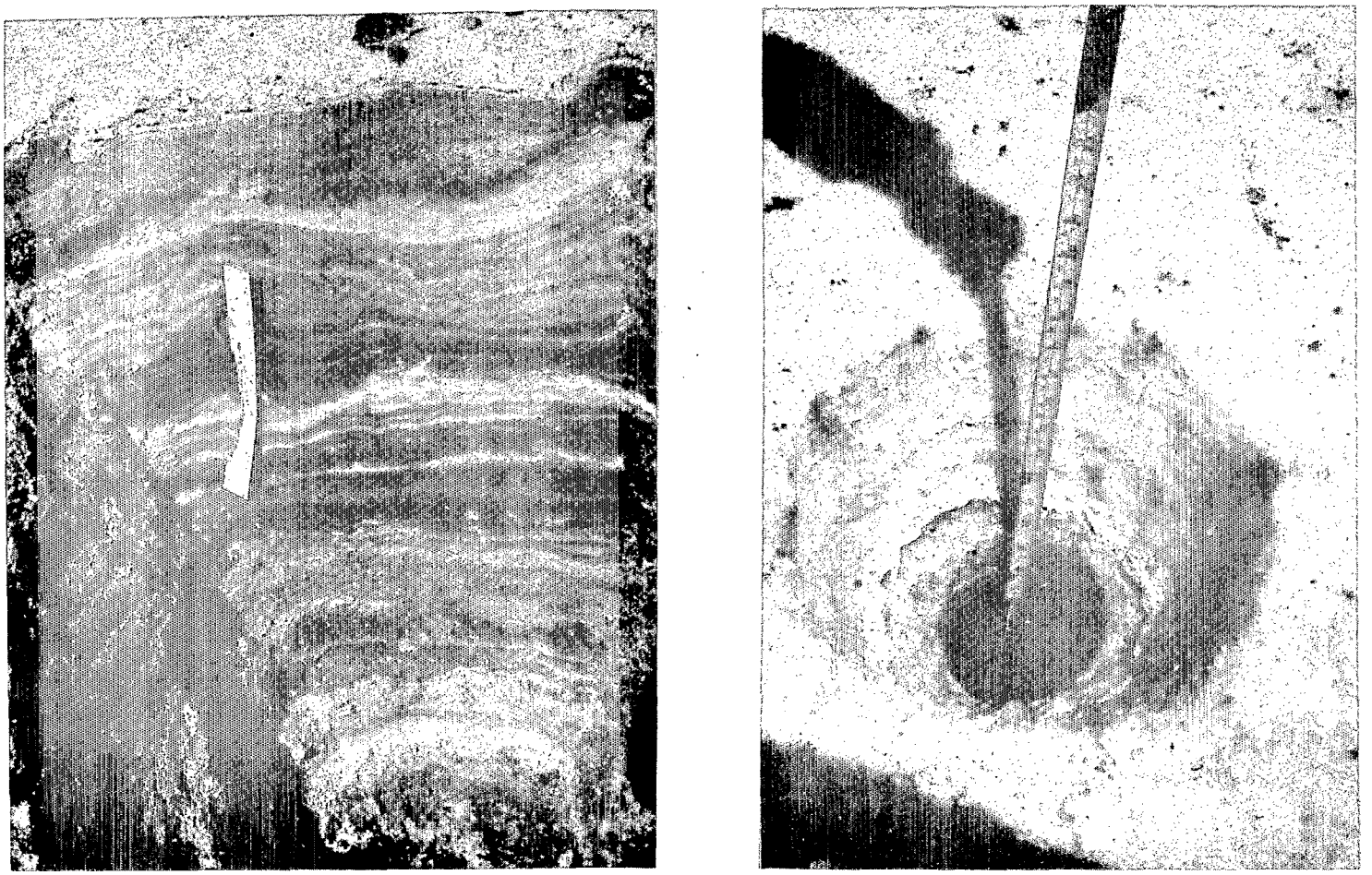

(a) (b)

Figure 6. Two sampling pits on the sabkha of Section A. (a) Near the border between algal flat and gypsum-salt flat (approximately 24820 in Fig. 4). The white layers are gypsum and the black layers are accumulation of organic material, including both salt grass and algal debris. Note the irregularity and discontinuity of the layering. Scale is 15 cm long. Reproduced from Holser (1979a), with permission of the Mineralogical Society of America. (b) On the central salt flat (approximately 24823 in Fig. 4). White layers are mainly halite and gypsum, gray layers still contain some organic material (grass, etc.), and the dead white layer near the bottom of the pit is polyhalite. Scale in inches. Reproduced from Holser (1966), with permission of the American Mineralogist.

Table 3. Chemical and Isotopic Analyses of Brines, mg/l[a]

	Standard Seawater	Beach 18093-2	Algal flat 18093-9	Algal flat 18093-11	Edge salt 18135-1	Gypsum-salt flat 18138-1	Gypsum-salt flat 18137-1	Gypsum-salt flat 18136-1	Gypsum-salt flat 18096-1
Na^+	11,100.	15,100.	42,200.	86,200.	70,500.	86,200.	68,000.	52,000.	29,400.
K^+	390.	607.	1,670.	4,500.	7,500.	5,700.	10,600.	11,500.	9,000.
Mg^{2+}	1,330.	1,960.	5,380.	30,000.	33,500.	21,400.	32,800.	52.500.	66,000.
Ca^{2+}	420.	943.	2,110.	370.	218.	126.	248.	130.	95.
Sr^{2+}	8.0	9.4	21.	8.0	8.0	6.4	4.	3.	<2.
Cl^-	19,800.	26,600.	82,000.	187,000.	189,000.	190,000.	191,000.	190,000.	200,000.
Br^-	66.	100.	270.	1,000.	1,400.	1,110.	1,650.	2,050.	3,200.
SO_4^{2-}	2,760.	5,600.	11,000.	31,500.	48,400.	30,700.	46,700.	59,500.	71,900.
δD, ‰	0.	+1.5	+1.6	+0.3	-2.0	-2.1	-2.1	-2.6	-3.0
$\delta^{34}S$, °/₀₀	+20.	+18.6			+18.8				+18.6
Density	1.025		1.095		1.242	1.212		1.262	1.265
Mean concentration[b]	1.0	1.47 ±0.05	4.24 ±0.04	19±4	24±2	16±1	26±1	36±5	50±1
Water table, cm	-	0	?	+3.	-1.	-30.	-6.	-1.	0.

[a]All from Section A of Figures 2, 3, 4, 5, except 18096-1 which is from Section B of Figure 2.

Analyses by conventional or atomic absorption methods by Gale Baker and Vina Spiehler, except for Sr by standard addition to optical emission spectrography by R. K. Wolven; δD by S. R. Silverman, all Chevron Oilfield Research Co. $\delta^{34}S$ by I. R. Kaplan (Holser & Kaplan, 1966).

[b]Mean concentration relative to seawater calculated by ratios of probably conservative elements.

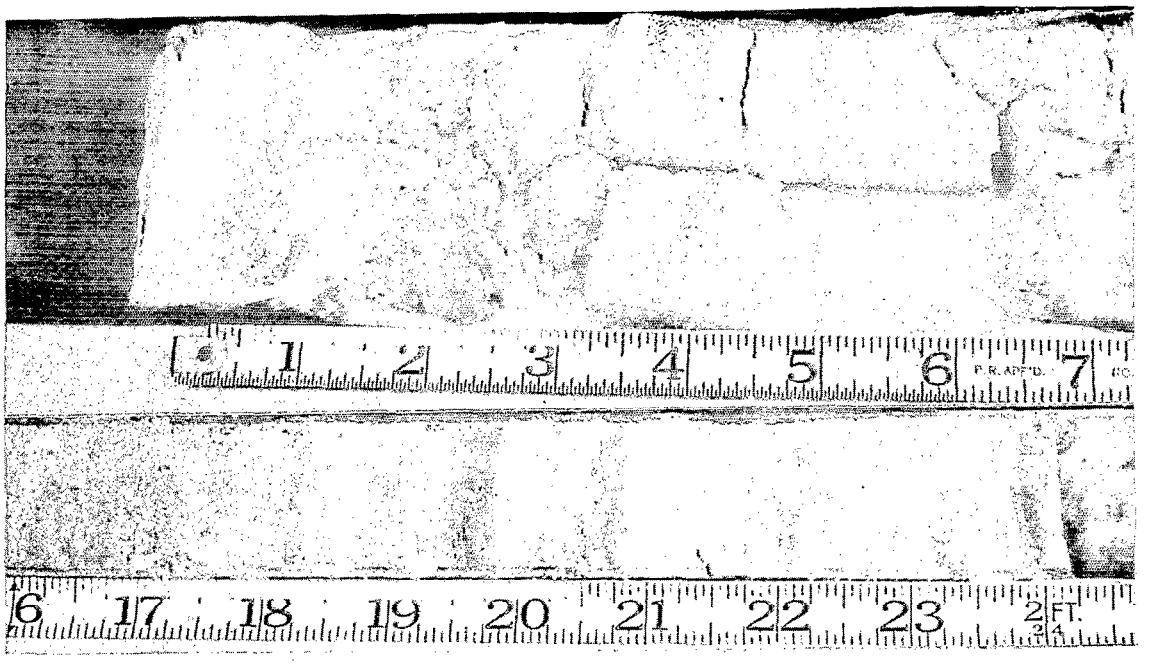

Figure 7. Two parts of the core from hole 18135 of Section A (Figs. 4, 5). Mixed halite and gypsum at top, with decreasing salt and increasing layering of organic debris downward. Scale in inches below surface. Reproduced from Holser (1979a), with permission of the Mineralogical Society of America.

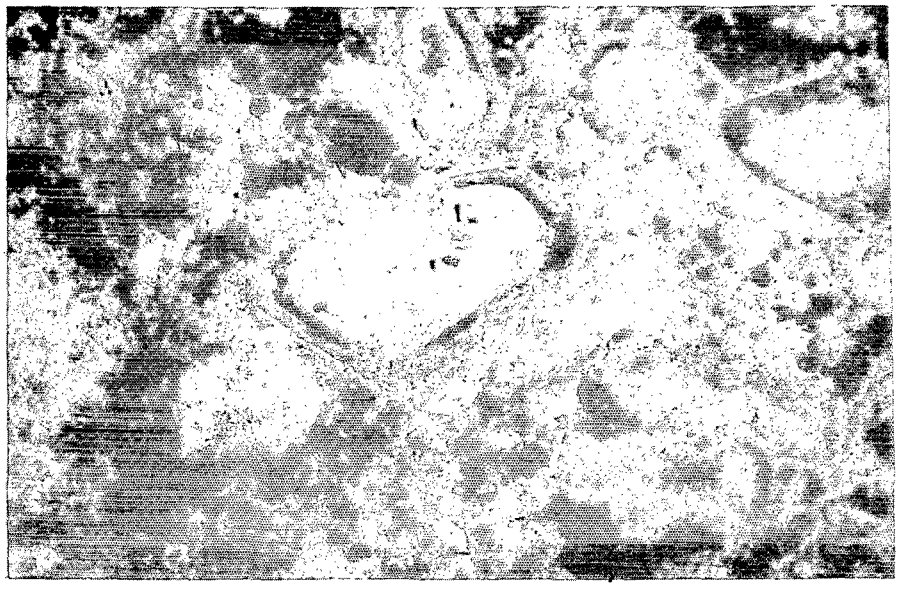

Figure 8. Photomicrograph (X40, plane-polarized light) of a rim of polyhalite replacing a euhedral gypsum crystal; most of the interstitial material is also polyhalite. Reproduced from Holser (1976), with permission of The American Mineralogist.

indicative rather than definitive, in view of the following recognized deficiencies: (1) Analyses of bicarbonate, alkalinity, pH, and Eh were not made: (2) Even allowing for a nominal amount of bicarbonate, the ionic balances are still off by ±2%; (3) The sampling is not isochronous, and the relevant data on tide, brine flow, temperature, and humidity are not recorded; and (4) Samples are mainly from brine in the more permeable of the layers just below the water table, but with an unknown contribution from deeper layers. The analyses given here are in some cases corrections of ones published previously (Holser, 1966; Holser & Kaplan, 1966).

In general, the brine analyses represent a series of increasing concentration, as modified by the crystallization and alteration of carbonates, gypsum, and halite; although the sequence does not exactly correspond to the geographical arrangement of Table 3. The analyses show the same general development as in the synchronous sequence from an extensive set of artificial brine pans analyzed in beautiful detail by Herrmann et al. (1973). It is significant that in both LOL and Herrmann's work, sulfate ion is concentrated and remains high through the highest evaporation stage. Taken with the sulfur isotope data (see below) this suggests that sulfate reduction is not quantitatively significant in either locality, despite the obvious reducing conditions under the algal mats at LOL and the negative Eh and zero O_2 content measured in the most concentrated pans by Herrmann et al. (1973). Consequently, the calcium and strontium levels in the brines (Sr was not measured by Herrmann et al.) are forced down to very low levels by precipitation of gypsum and celestite. At the same time, the rise of K and Mg forces the replacement of earlier gypsum by polyhalite. Chloride levels off when halite starts to precipitate, but bromide continues to rise (although at a slower rate) by virtue of its rejection from halite. But the most concentrated brine is not at a level sufficient to expect minerals of the potash-magnesia facies (e.g., Holser, 1979a).

Isotope Geochemistry

Sulfur isotope geochemistry of brines and sulfate minerals along section A was reported in detail by Holser and Kaplan (1966), including specific sample descriptions. In general, the brines are remarkably uniform in composition at $\delta^{34}S = +18.7 \pm 0.1‰$. Any quantitatively important bacterial reduction of sulfate to sulfide, in the brines, would have pushed the $\delta^{34}S$ upward from the normal sea water value of +20‰. The levels determined, including water from the lagoon itself, are about 1‰ lighter than normal for present sea water. Although specific data on $\delta^{34}S$ in sulfate of continental ground water of this area is not available, continental waters are usually lighter in $\delta^{34}S$ than sea water. The low $\delta^{34}S$ could possibly indicate a minor admixture of such continental sulfate in the brines and lagoon. The sulfate minerals from a variety of occurrences in the evaporite deposit (10 analyses) have $\delta^{34}S = +21.0 \pm 0.7‰$. The levels are 1-2‰ heavier than sea water or the lagoon water, as expected from a slight fractionation during crystallization (for a critical review see Claypool et al., 1980). Polyhalite is not significantly different from gypsum.

Deuterium levels were measured in some brine samples--unfortunately, it was not possible to combine these analyses in the usual way with measurements of oxygen isotopes. The results (previously summarized in Holser, 1979b) are given in Table 3. Evaporation of the brine initially causes a

rise in δD, but at higher salinities a sharp reversal towards lighter δD occurs, in accord with the experimental and theoretical results of Gonfiantini (1965) and Gat (1980). The decrease in δD landward could either be due to this type of evaporative reversal, or alternatively it could be due to dilution by customarily light continental ground waters. It is possibly significant that the sequence of δD is ordered more closely with the geographic sequence of Table 3 (see Fig. 4) than it is with the various determinations of the degree of concentration of salts expressed in the data of Table 3. Perhaps this indicates that the waters of the brines have been subjected to a uniform increase of evaporative stage from west to east (or uniform mixing with continental waters), whereas the chemistry of their dissolved constituents may have been modified by re-solution or alteration of previously deposited minerals.

Discussion

The expected characteristics of the LOL sabkha, and in particular of Section A, are:

(1) A general increase from shore towards the land of degree of evaporation, of density, and of concentration of conservative chemical elements in the brines permeating the sabkha.

(2) A consequent shift from carbonate mineralogy to higher evaporite mineralogy.

(3) The alteration of HMC and probably aragonite to dolomite.

The unusual or unexpected aspects of this sabkha are:

(4) The widespread and permanent deposition of halite, in contrast to only minor or evanescent (or absent) halite in many other Recent sabkhas.

(5) The failure of gypsum and halite to separate as distinct depositional facies.

(6) The high concentration of the brines, and the consequent alteration of gypsum to polyhalite, and deposition of (alteration of HMC to?) magnesite.

(7) The absence of alteration of gypsum to anhydrite (or of direct precipitation anhydrite), in spite of the low activity of H_2O in the brines of high concentration and temperature.

(8) The absence of substantial sulfate reduction. While this may be unexpected in the face of common ad-hoc models of sabkha chemistry, it is in complete accord with the fact that most gypsum rocks in the sedimentary section, including most ancient sabkhas, have sulfur isotope ratios that correlate synoptically around the world. Such sulfates are therefore presumed to be samples of sea water and not of sulfates variably increased in $\delta^{34}S$ by local basinal sulfate reduction (e.g., Claypool et al., 1980).

MINERALOGY AND GEOCHEMISTRY OF SABKA SEDIMENTS AND BRINES: SECTIONS E_1 & E_2 (C.P.,L.O.)

Sedimentary Deposits

(See Figs. 9, 10 and 11)

Along the southern coast of Ojo de Liebre lagoon, extensive salt-marshes cut by numerous tidal-channels, are backed by supratidal flats, covered by a thin algal-mat. This algal-mat shows polygonal structures and progressively disappears landwards. The surface is strewed with dried algae (Zostera marina) and marine shells (mainly Melampus olivaceous) which are carried by the wind and the highest spring tides. Sections E_1 and E_2 were studied at, respectively, 10 and 11 Km from the pump station, across the supratidal flats.

Carbonate sediments have a maximal thickness of 45 cm (Fig. 10,11); they are located in the external part of the flats below the algal-mat. Two macrofacies may be distinguished: the upper layer with a yellowish colour is pelloid, while the lower light grey layer is finely grained. Drift shells and plant remains are observed in these deposits.

Carbonate sediments are underlain by gypsum in section E_1 (Fig.11) or by sand in Section E_2 (Fig. 10); landwards, they laterally grade to gypsum deposits. The gypsum crystals have a lenticular habit which indicates a crystallization by diagenetic emplacement in the host sediments (Shearman, 1971). They frequently present dissolution features and, just below the surface, nodular recrystallizations. At the landward edge of the flat, gypsum crystals are accumulated by winds and form gypsum dunes.

Mineralogy of Carbonates

The carbonate fraction of these deposits consists of a complex assemblage of rhombhoedral carbonates, sometimes with aragonite (Pierre and Person, in press). This aragonite, detected by X-ray analysis, is mainly related to the presence of shell fragments, but may also be represented by needles (observed in smear slides) of primary precipitation. The chemical composition of rhomboedral carbonates was determined by X-ray diffraction measurements, using the idealized curve of Goldsmith and Graft (1958). In some samples this composition may be difficult to determine, particularly when the diffraction picks are not well separated.

The main carbonate phase corresponds to magnesian calcites with 14 to 16 moles % $MgCO_3$. It may be associated with a low-magnesian calcite (6 moles% $MgCO_3$) and with a high-magnesian calcite (up to 25 moles% $MgCO_3$) (Table 5).

Other magnesium-rich rhomboedral carbonates are associated with magnesian calcites; they preferentially occur in sediments below and just above the water table. Their chemical compositions range from $(Ca_{70}Mg_{30})$ to $(Ca_{55}Mg_{45})$; therefore they may be considered as calcian dolomites.

Interstitial solutions: physico-chemical data

(See Table 4)

Interstitial solutions show increasing densities in a landward direction ($1,047 < d < 1,092$); these densities correspond to dissolved salt contents ranging from about 80 to 180 g/Kg and furthermore indicate that solutions are probably under- saturated relative to gypsum, since gypsum saturation of a marine brine is reached for densities close to 1, 110. This interpretation is in agreement with dissolution features observed in gypsum crystals.

Temperatures of the interstitial solutions are quite constant ($t = 20 \pm 1,5°C$) all along the sections.

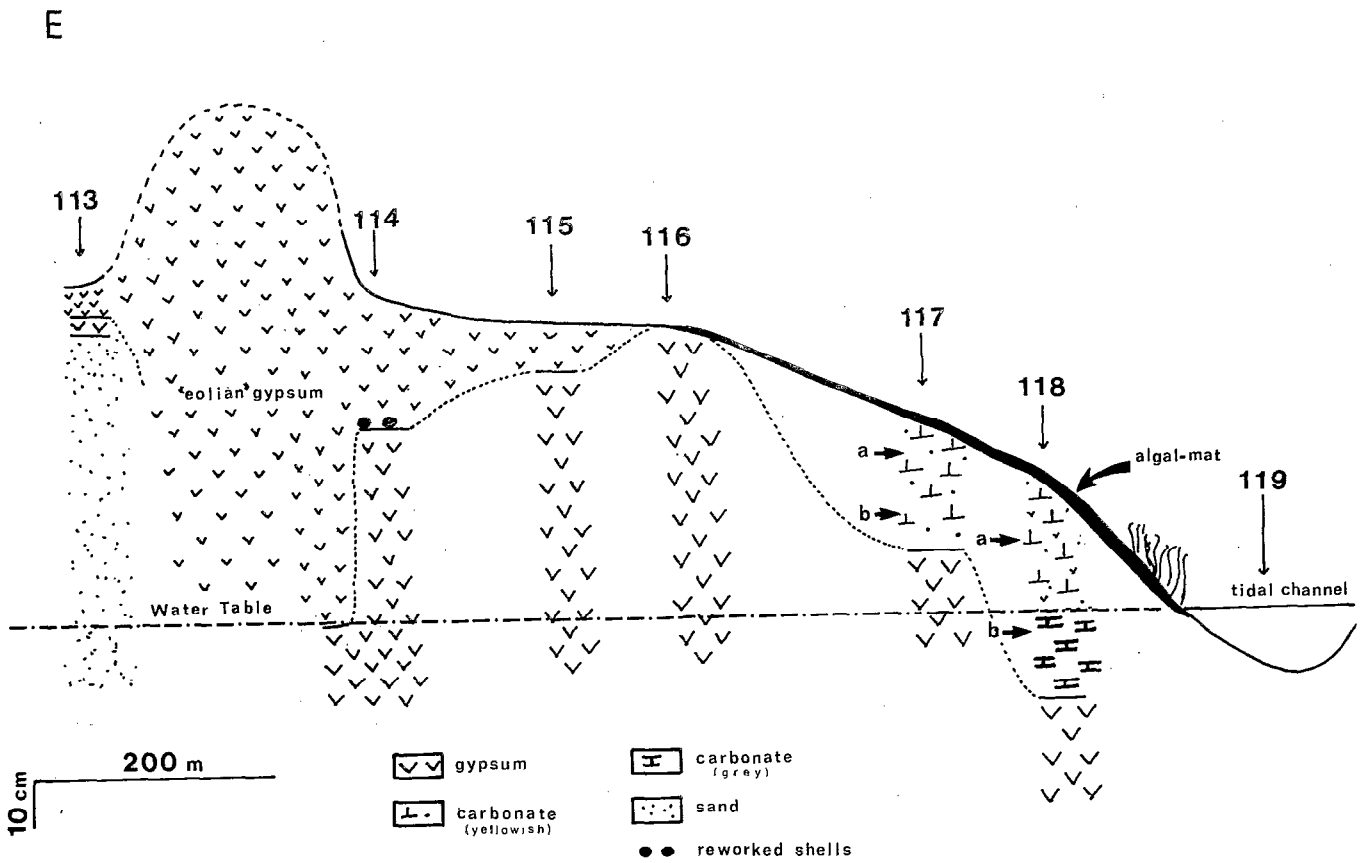

Figure 10. CROSS-SECTION E_1 OF THE SUPRATIDAL FLAT ON THE SOUTHERN SHORE OF OJO DE LIEBRE LAGOON: SAMPLES 113 TO 119 (SEE FIG. 9 FOR LOCALIZATION).

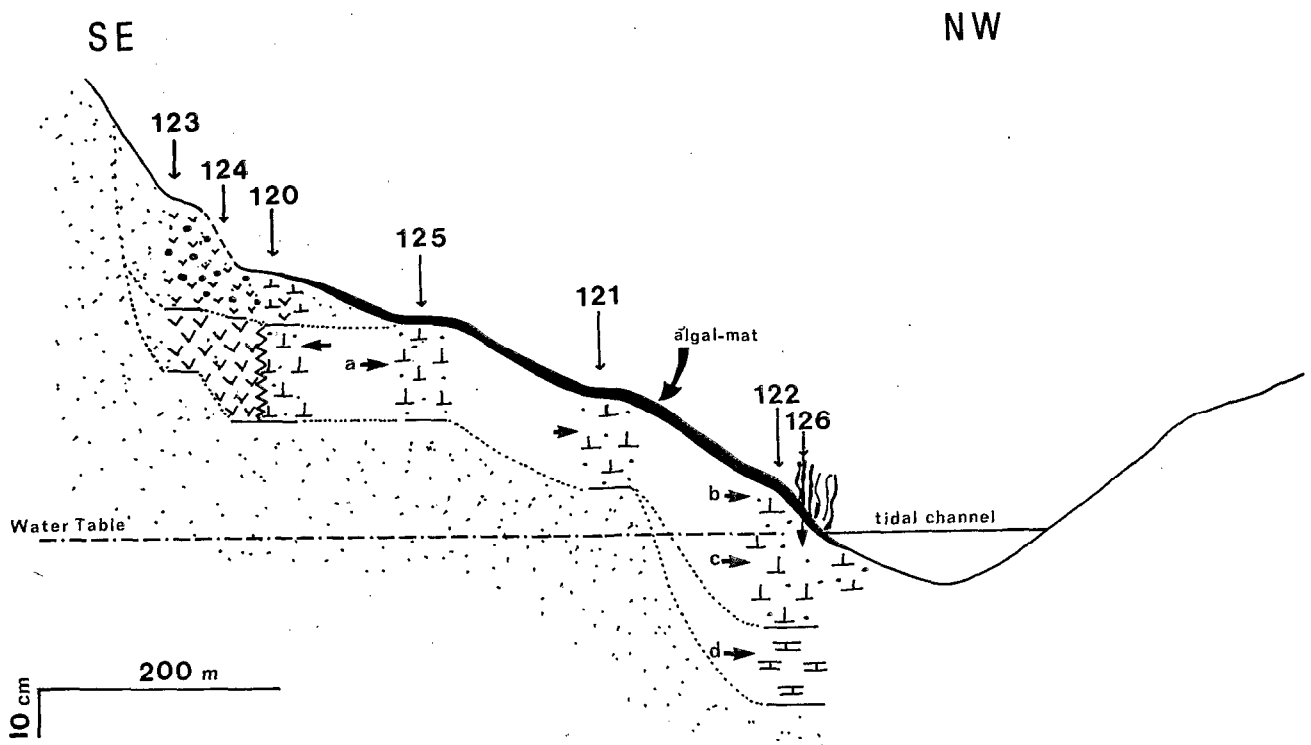

Figure 11. CROSS-SECTION E_2 OF THE SUPRATIDAL FLAT ON THE SOUTHERN SHORE OF OJO DE LIEBRE LAGOON: SAMPLES 120 TO 126 (SEE FIG. 10 FOR LEGEND, AND FIG. 9 FOR LOCALIZATION).

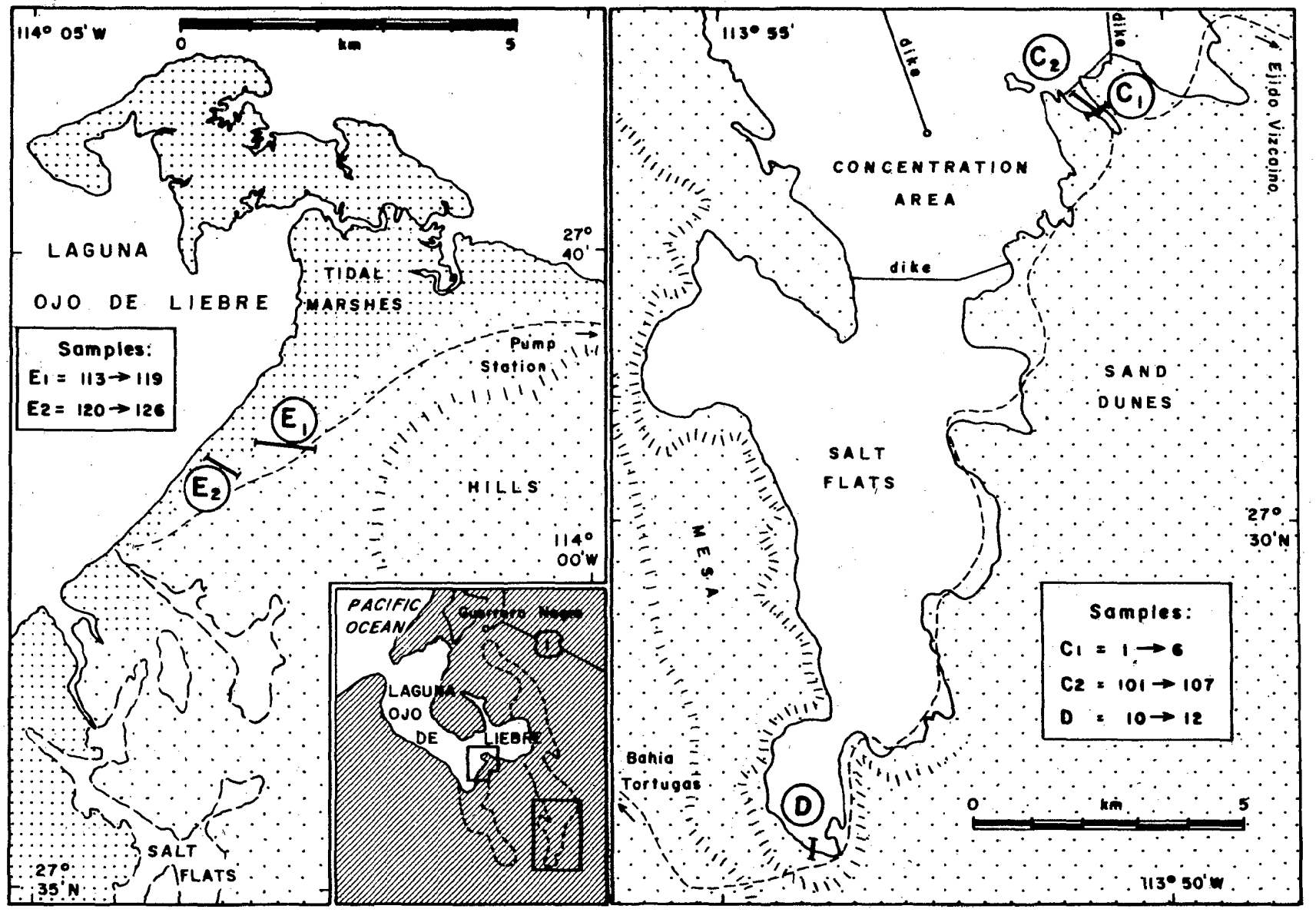

Figure 9. Localization of the analyzed samples in sections C_1, C_2, D, E_1 and E_2 in the southern area of Ojo de Liebre complex.

Table 4 = Physico-chemical and isotopic data on interstitial brines from supratidal flats on the southern shore of Ojo de Liebre Lagoon

	density	pH	Eh (mV)	t°C	$\delta^{18}O$/SMOW
L 113	1.078	7.2	+350	20.5	+1.4
L 114	1.090	7.75	+330	21.5	+1.57
L 115	1.092	7.75	+260	21	+1.74
L 116	1.091	7.6	+350	21.5	+2.47
L 117	1.086	7.6	+310	21.5	+2.27
L 118	1.069	7.15	+270	21	+2.57
L 119	not measured (collected in a tidal-channel)				+3.60
L 123	1.079	7.25	+370	21.5	+2.20
L 124	1.069	7.4	+320	20	+2.20
L 120	1.087	7.3	+430	21.5	+2.50
L 125	1.080	7.3	+330	21.5	+2.60
L 121	1.058	7.5	+320	19	+2.40
L 122	1.047	7.1	+40	19	+2.60

Table 5 = Mineralogy and isotope contents of carbonates from supratidal flats on the southern shore of Ojo de Liebre Lagoon

Sample	Associated minerals	Calcite (mole % $MgCO_3$)	Dolomite (mole % $MgCO_3$)	$\delta^{18}O$ / P.D.B. (bulk carbonate)	$\delta^{13}C$ / P.D.B. (bulk carbonate)
L 117a		Mg_{15}	Mg_{36}	+1.8	+2.0
L 117b	gypsum	Mg_{15}	--	+1.4	+1.5
L 118a	gypsum aragonite	Mg_{14}	Mg_{35} Mg_{38} Mg_{44}	+2.0	+2.2
L 118b	aragonite	Mg_{14} Mg_{15} Mg_{23}	Mg_{46}	+2.2	+2.2
L 120		Mg_{12}	--	+0.9	+1.7
L 125a	aragonite	Mg_{15}	Mg_{31}	+2.6	+2.7
L 121	aragonite quartz feldspath	Mg_3 Mg_{14}	- -	+1.8	+3.0
L 122b	quartz feldspath	Mg_{13} Mg_{24}	Mg_{38}	+1.6	+0.2
L 122c	quartz feldspath	Mg_{14} Mg_{28}	Mg_{43}	+2.4	+0.1
L 122d	quartz feldspath	Mg_{14}	Mg_{43}	+2.3	-0.3
L 126	quartz feldspath	Mg_5 Mg_{11}	Mg_{45}	+1.8	-0.9

Variations in pH values are slight (7,20 pH 7,75). Redox potentials (Eh) have very high values (+ 260 mV< Eh <+ 430 mV) which characterize oxidizing conditions. At the salt-marsh edge, the low Eh value (Eh= + 40 mV) shows that slightly reducing conditions are occurring; this is also marked by the presence of free H_2S in the water.

Stable isotopes geochemistry

(See Tables 4 and 5)

Isotopes contents were measured in interstitial solutions for ^{18}O, and in bulk carbonate for ^{18}O and ^{13}C.

Although densities are increasing landwards, $\delta^{18}O$ values of solutions are almost constant, with an average value of + 2, 5 °/₀₀ (Fig. 23). At the landward edge of the flat, both ^{18}O and salt contents are decreasing. These data indicate that marine derived brines may be diluted by continental groundwaters. Thus, part of the mineralization of solutions is probably related to gypsum dissolution.

A direct correlation is observed between the highest $\delta^{18}O$ values in the bulk carbonate and the occurrence of dolomite. Therefore, dolomitization was probably accompanied by an oxygen isotope enrichment relative to calcite which might crystallize in the same conditions (Pierre and Person, in press.). Many authors (Clayton & Epstein, 1958; Clayton et al; 1968; Engel et al; 1958; Fontes et al, 1967, 1969, 1970; Fontes & Perthuisot,1971; Fritz & Smith; 1970; Matthews & Katz, 1977) have shown the existence of a dolomite-calcite ^{18}O fractionation (by 3 to 4 °/₀₀ at sedimentary temperatures) during the process of early dolomitization. It hence appears that dolomite crystallization at Ojo de Liebre is due to a very early diagenesis of a magnesian precursor; it is carried out via intermediate phases of high magnesian calcites.

^{13}C contents of the carbonates indicate that their crystallization occurred either under the control of the oceanic reservoir in equilibrium with atmospheric CO_2 ($\delta^{13}C$ = + 2 °/₀₀), or in a semi-restricted environment where HCO_3 is partly biogenic (- 0, 9 °/₀₀ < $\delta^{13}C$ <+ 0,2 °/₀₀). Furthermore, carbonate samples with low $\delta^{13}C$ values correspond to the lowest redox potentials measured in interstitial solutions.

Conclusions

Carbonate sediments from the supratidal flats of the southern shore of Ojo de Liebre lagoon are submitted to a very early diagenesis which leads to the formation of magnesian calcites and dolomites. Calcite represents the dolomite precursor, and interstitial solutions provide the magnesium required for the mineral transformation.

MINERALOGY AND GEOCHEMISTRY OF SABKA SEDIMENTS AND BRINES: SECTION D (C.P.,L.O.)

Sedimentary deposits

(See Figs. 9 and 12)

The inner salt pan of the southernmost part of Ojo de Liebre complex is surrounded by a mesa about 20 metres high (Ortlieb and Pierre, in prep.) The Section D is located on the southern margin of this southernmost supratidal area of the Ojo de Liebre complex (Fig.9). The distribution of evaporites follows a circular pattern (bull's eye structure): halite deposits occupy the centre of the pan and gypsum deposits are located along the basin edge(Fig.12).

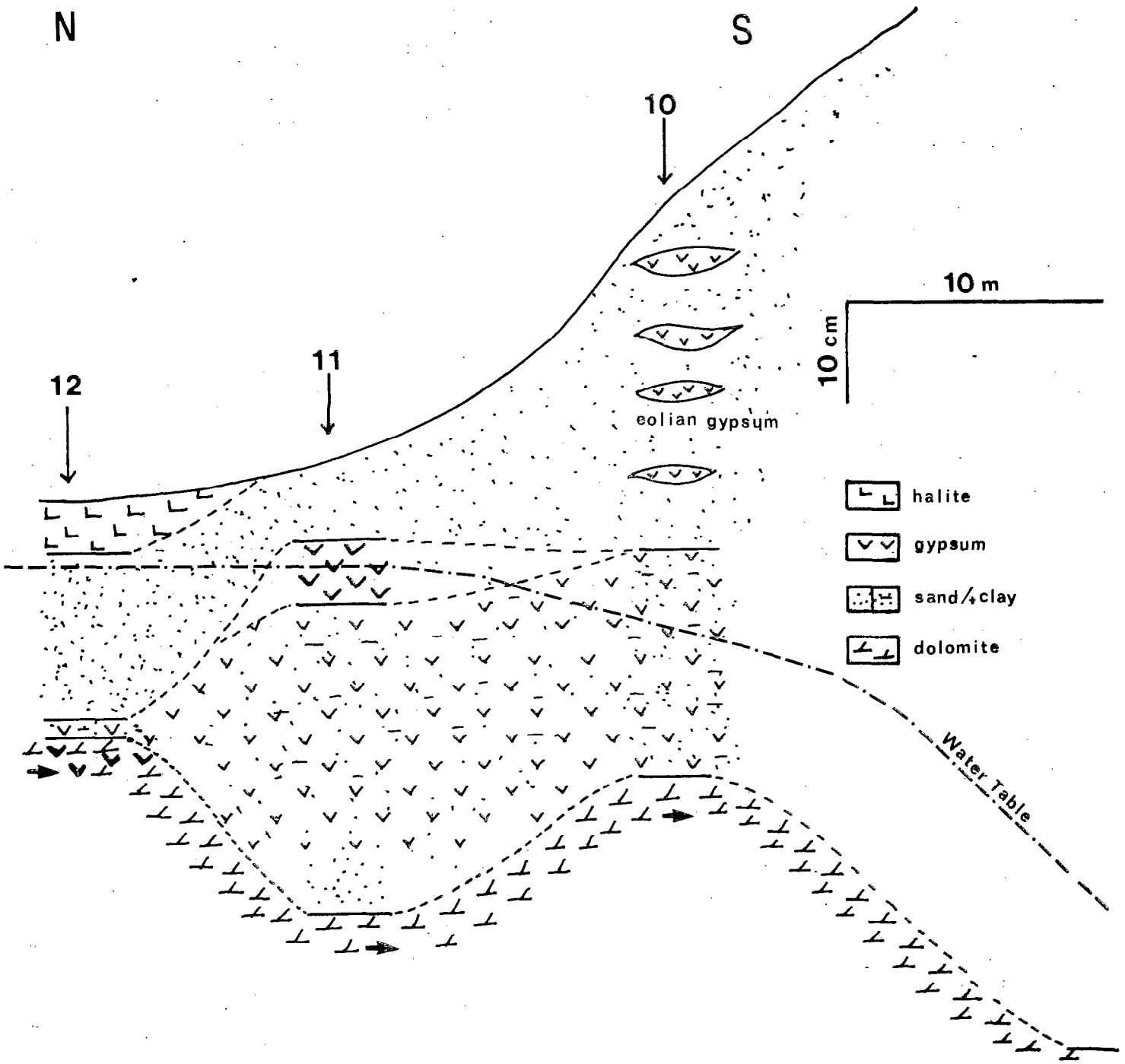

Figure 12. Cross-section D at the southern edge of the southernmost salt pan in Ojo de Liebre complex: samples 10, 11 and 12 (localization Fig. 9).

Gypsum crystals commonly have a lenticular habit which indicates that they have displacively grown in the host detrital sediment (Shearman, 1971). These crystals may be reworked by the wind and are locally accumulated at the base of the cliff. The gypsum deposits are underlain by a marly green sediment which contains a few large lensoid crystals of gypsum.

Mineralogy of sediments

Diagenesis in sediments from this locality is clearly demonstrated by their mineralogy. X-ray diffraction analysis show that the lower marly layer is almost entirely constituted by pure dolomite, with 5 moles % excess $MgCO_3$ in the crysta lattice. In spite of the lack of $CaCO_3$ in the sedimentary sequence, dolomitization was probably induced by the complete transformation of a $CaCO_3$ precursor with surrounding solutions enriched in magnesium. The dolomitization is accompanied by the crystallization of large gypsum crystals.

Interstitial solutions: physico-chemical data

(See Figs. 13 to 19 and Table 5)

Salt contents in interstitial brines increase while pH values decrease (in response to lower water activities) towards the centre of the pan. Redox potentials are positive although more reducing conditions predominate in the centre of the basin (where a sharp decrease in Eh, of more than 200 mV, is registered).

Concentrations in ionic species of the interstitial solutions do not correspond to normal marine brines. (K^+) and (Mg^{2+}) concentrations sharply increase in the centre of the basin where solutions have the highest densities. Total alcalinities are very low. (SO_4^{2-}) and (Ca^{2+}) concentrations respectively decrease and increase when densities are increasing. These results are in good agreement with the diagenesis expressed in the sediments: (Mg^{2+}) is used during dolomite formation while released (Ca^{2+}) reacts with (SO_4^{2-}) to form gypsum.

Stable isotopes geochemistry

(See Figs. 20 and Tables 6 and 7)

Isotopic analysis were carried out on both waters and dolomites. $\delta^{18}O$ values in waters are lower than for evaporated marine waters ($-0{,}2\ ‰ < \delta^{18}O < +1{,}3\ ‰$); they are most probably due to a dilution of marine brines by continental waters.

Heavy isotopes contents in dolomites are very high for ^{18}O ($+3{,}0\ ‰ < \delta^{18}O < +3{,}8\ ‰$) and are low for ^{13}C ($-5{,}3\ ‰ < \delta^{13}C < -3{,}7\ ‰$). $\delta^{18}O$ values indicate that dolomitization was accompanied by an oxygen isotope enrichment (close to 3,7 ‰) relative to calcite which might crystallize in the same environmental conditions (temperature and $\delta^{18}O$ of water); as a result, these dolomites appear to have crystallized in an early stage of diagenesis.

Low $\delta^{13}C$ values show that large inputs of biogenic CO_2 were provided during the dolomitization process. Lippmann (1973) previously emphasized the importance of biogenic activity in dolomite formation since increasing alcalinities enhance the reaction.

Conclusions

The diagenesis which arises in the evaporitic sequence of the southernmost part of the Ojo de Liebre complex corresponds to an early dolomitization. The reaction leads to the complete transformation of an inferred $CaCO_3$ precursor by magnesium-rich solutions. The mineral transformation was accompanied by an oxygen isotope enrichment and was probably supported by inputs of biogenic CO_2.

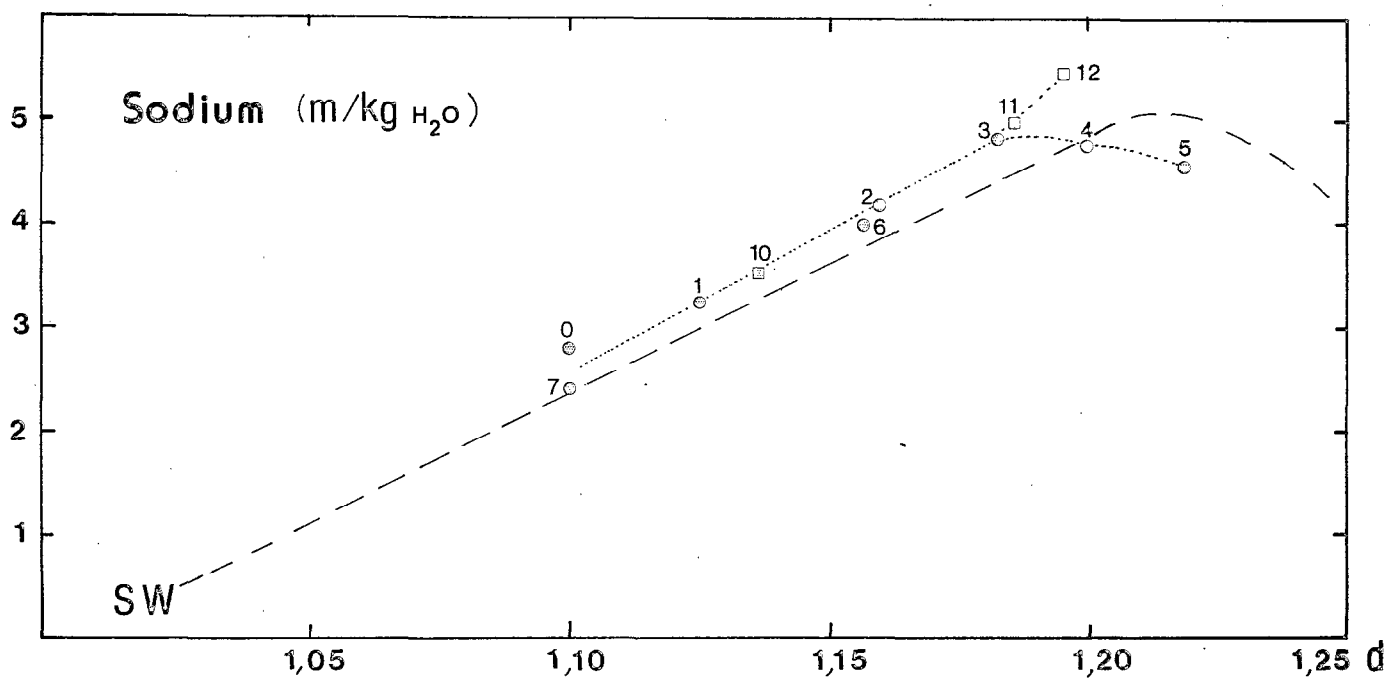

Figure 13. VARIATIONS IN (Na^+) CONCENTRATIONS, EXPRESSED IN MOLALITIES, RELATIVE TO DENSITY IN INTERSTITIAL SOLUTIONS (SECTIONS C_1 AND C_2); EVOLUTION OF SEA WATER (SW) DURING EVAPORATIONS IS GIVEN BY COMPARISON.

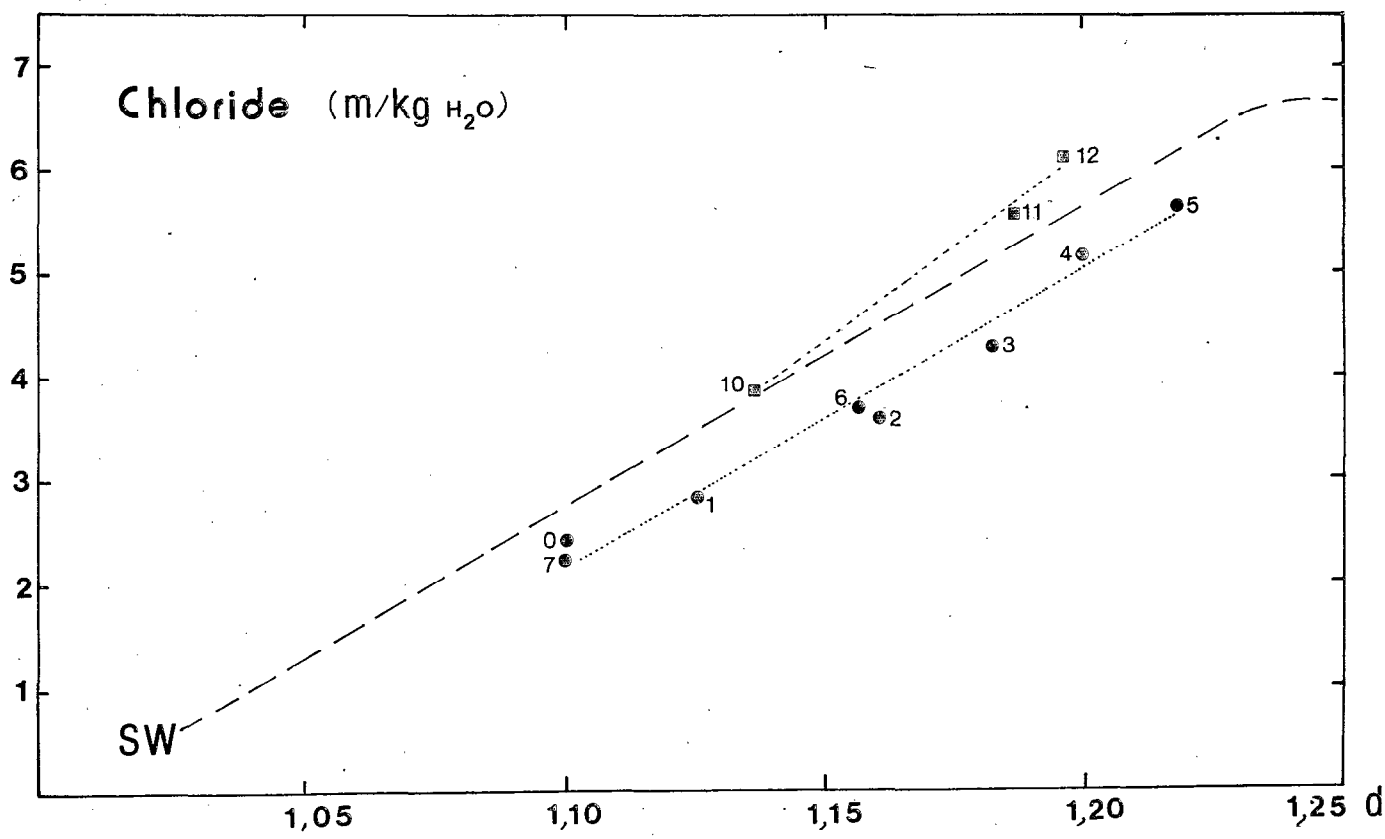

Figure 14. VARIATIONS IN (Cl^-) CONCENTRATIONS, EXPRESSED IN MOLALITIES, RELATIVE TO DENSITY IN INTERSTITIAL SOLUTIONS (SECTIONS C_1 AND C_2); EVOLUTION OF SEA WATER DURING EVAPORATION IS GIVEN BY COMPARISON.

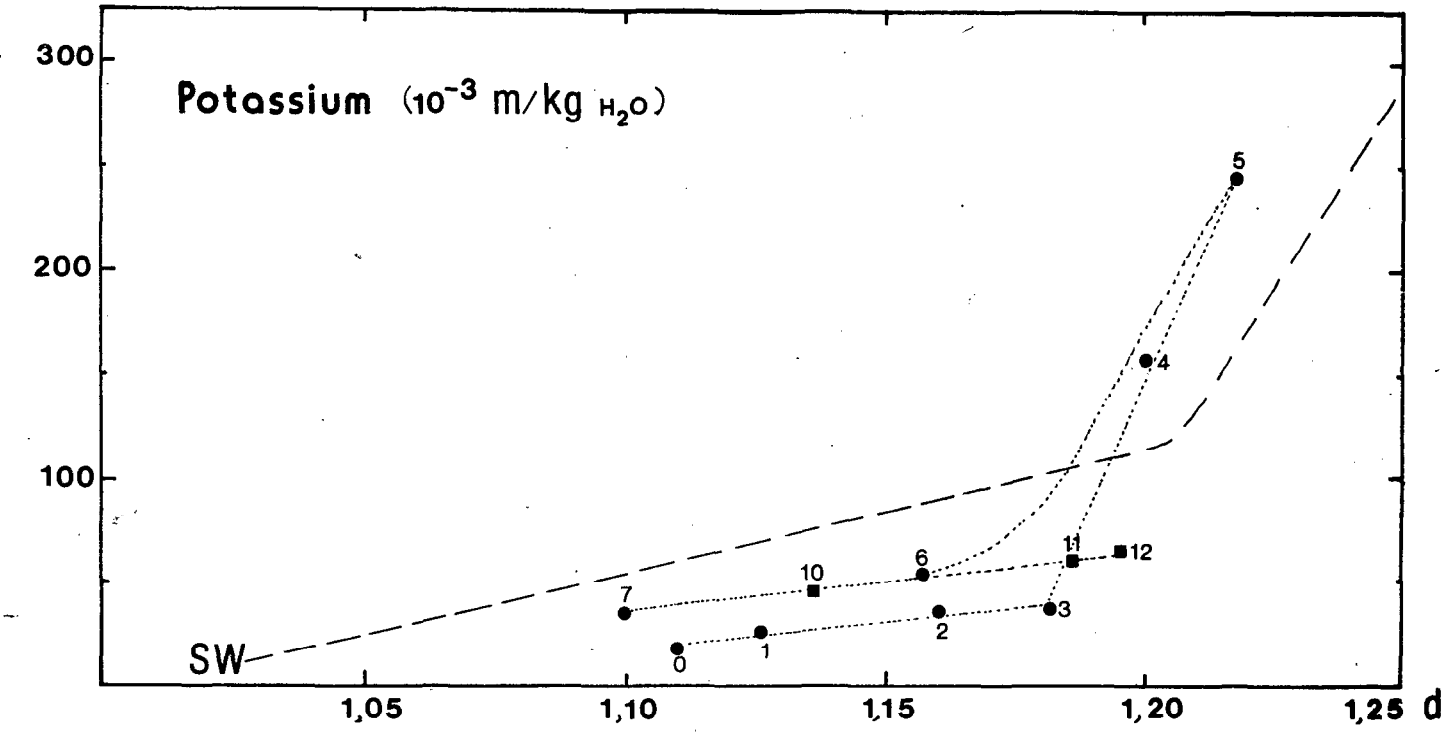

Figure 15. VARIATIONS IN (K^+) CONCENTRATIONS, EXPRESSED IN MOLALITIES, RELATIVE TO DENSITY IN INTERSTITIAL SOLUTIONS (SECTIONS C_1 AND C_2); EVOLUTION OF SEA WATER DURING EVAPORATION IS GIVEN BY COMPARISON.

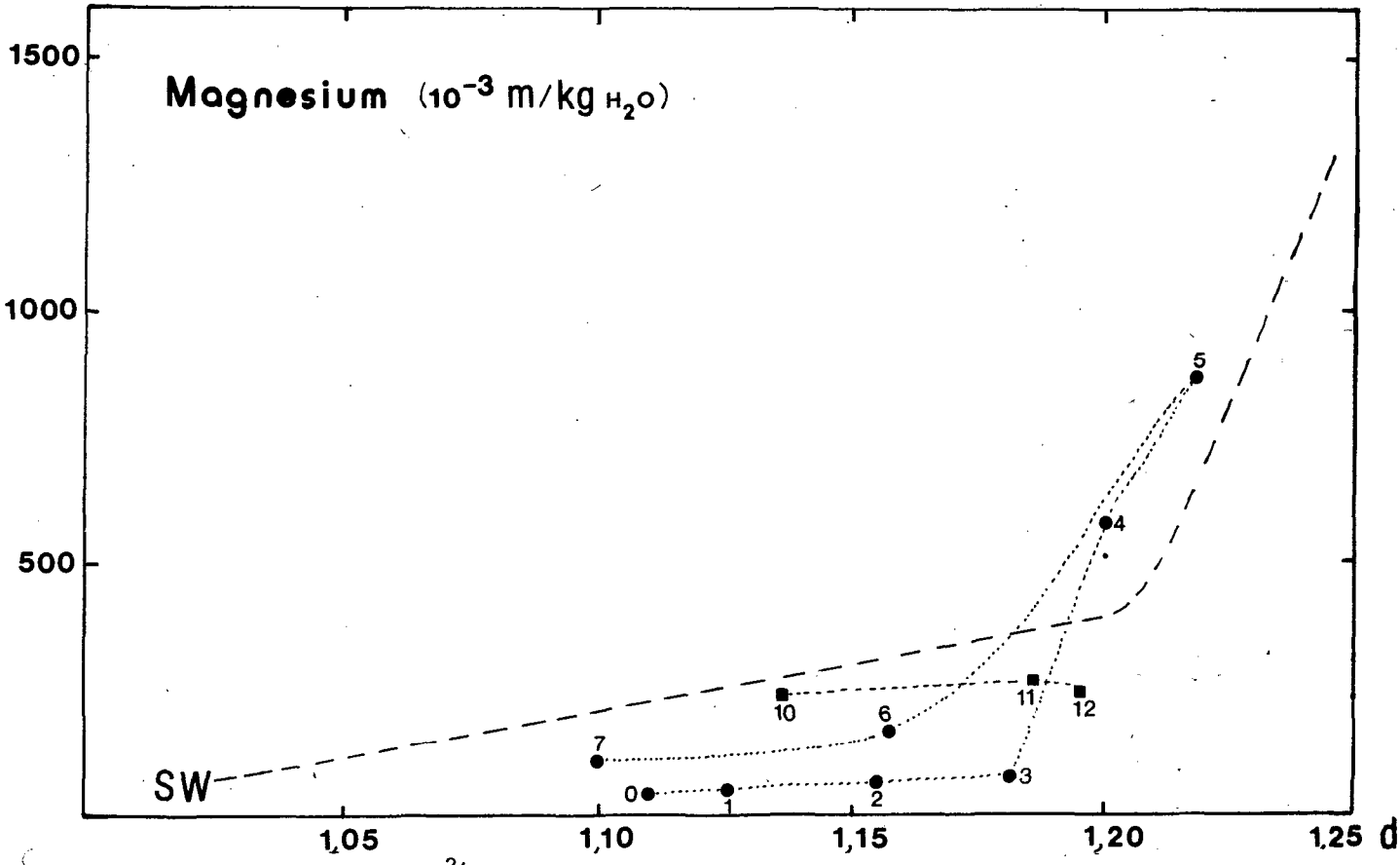

Figure 16. VARIATIONS IN (Mg^{2+}) CONCENTRATIONS, EXPRESSED IN MOLALITIES, RELATIVE TO DENSITY IN INTERSTITIAL SOLUTIONS (SECTIONS C_1 AND C_2); EVOLUTION OF SEA WATER DURING EVAPORATION IS GIVEN BY COMPARISON.

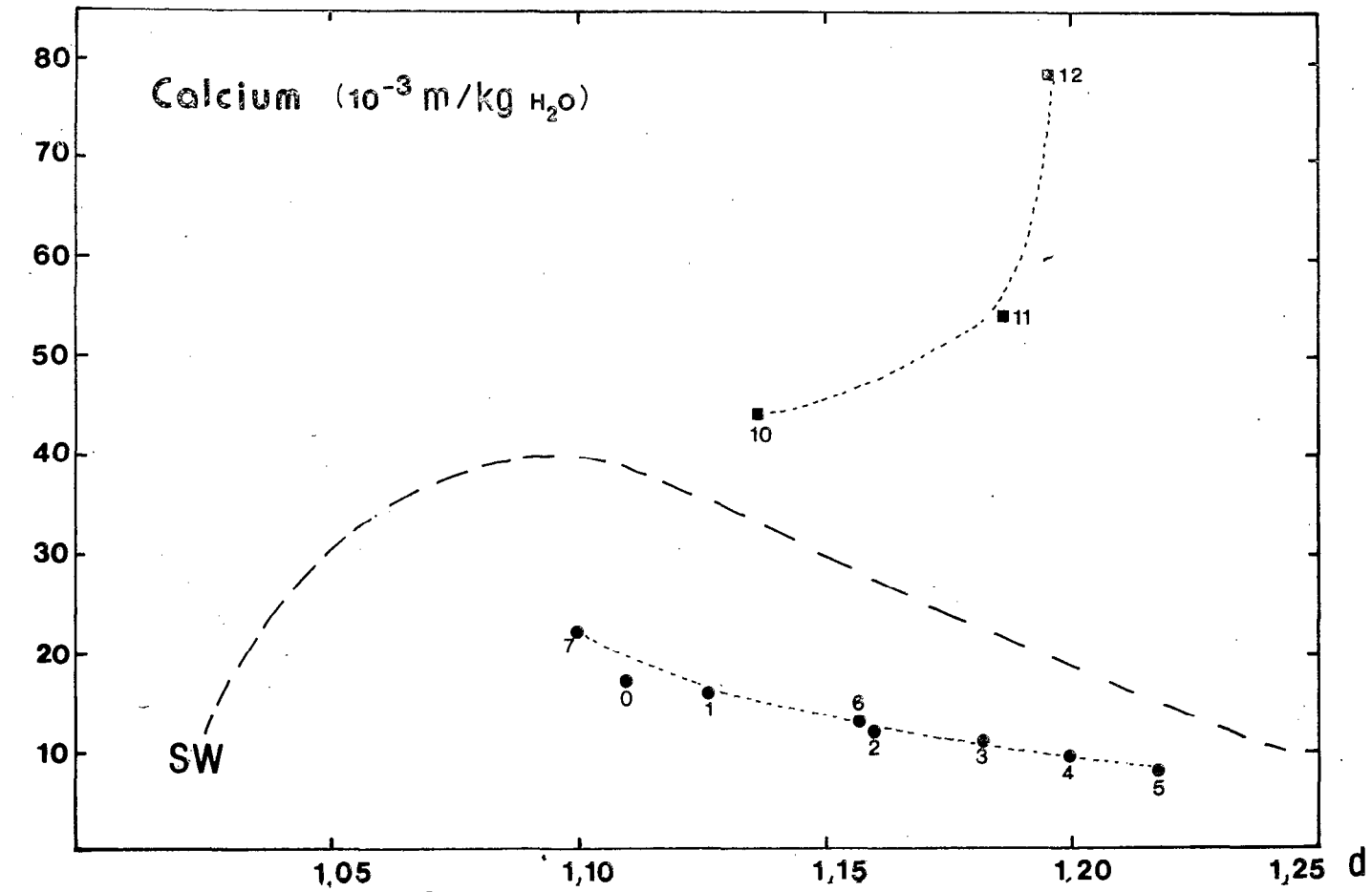

Figure 17. VARIATIONS IN (Ca^{2+}) CONCENTRATIONS, EXPRESSED IN MOLALITIES, RELATIVE TO DENSITY IN INTERSTITIAL SOLUTIONS (SECTIONS C_1 AND C_2); EVOLUTION OF SEA WATER DURING EVAPORATION IS GIVEN BY COMPARISON.

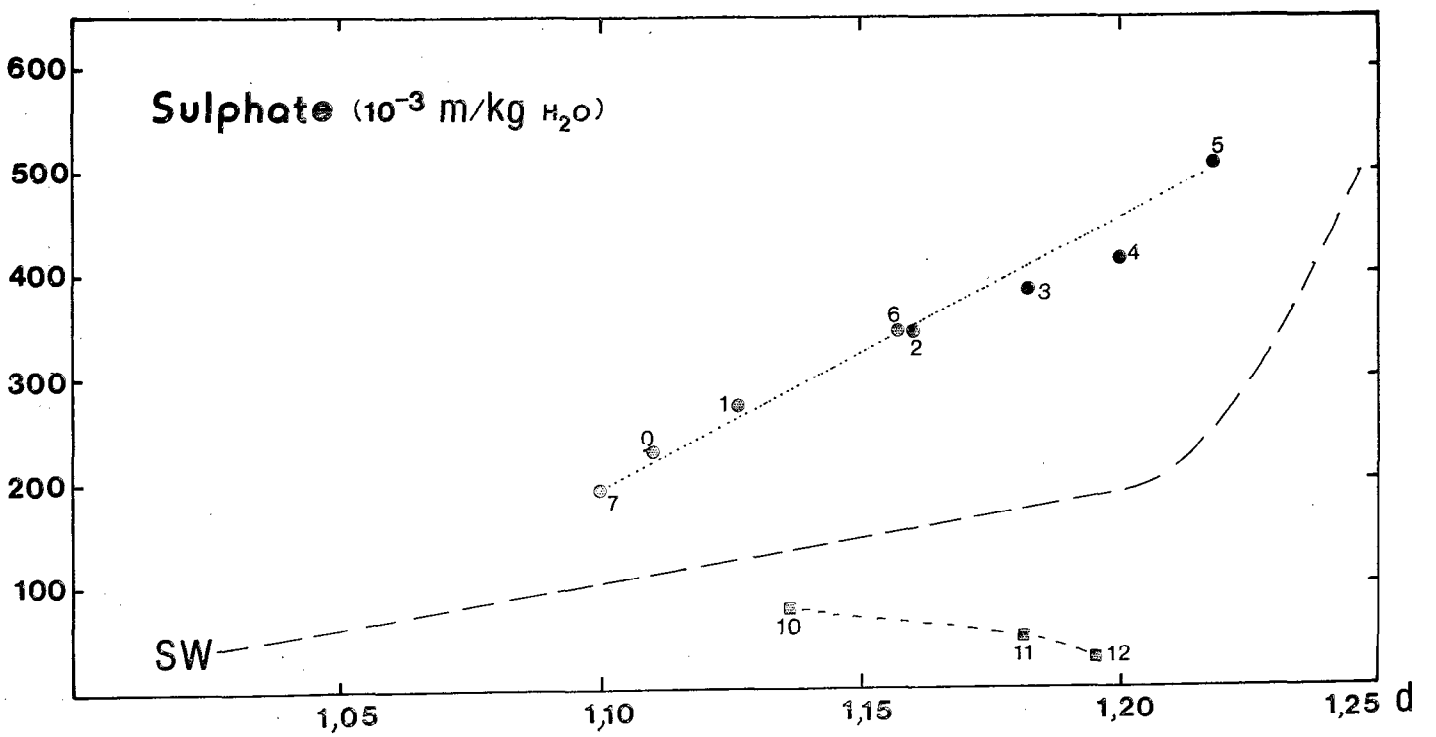

Figure 18. VARIATIONS IN (SO^{2-}) CONCENTRATIONS, EXPRESSED IN MOLALITIES, RELATIVE TO DENSITY IN INTERSTITIAL SOLUTIONS (SECTION C_1 AND C_2); EVOLUTION OF SEA WATER DURING EVAPORATION IS GIVEN BY COMPARISON.

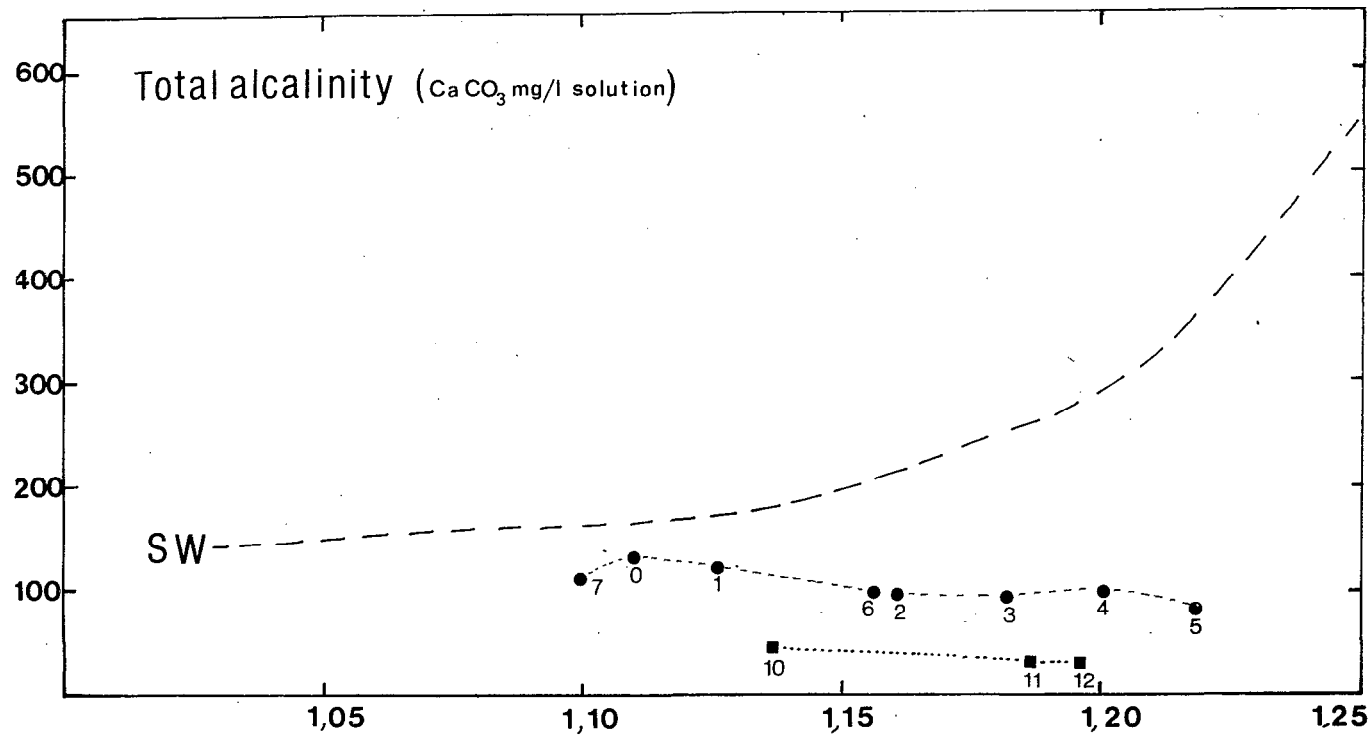

Figure 19. VARIATIONS IN TOTAL ALCALINITY, EXPRESSED IN $CaCO_3$ MOLARITIES, RELATIVE TO DENSITY IN INTERSTITIAL SOLUTIONS (SECTIONS C_1 AND C_2); EVOLUTION OF SEA WATER DURING EVAPORATION IS GIVEN BY COMPARISON.

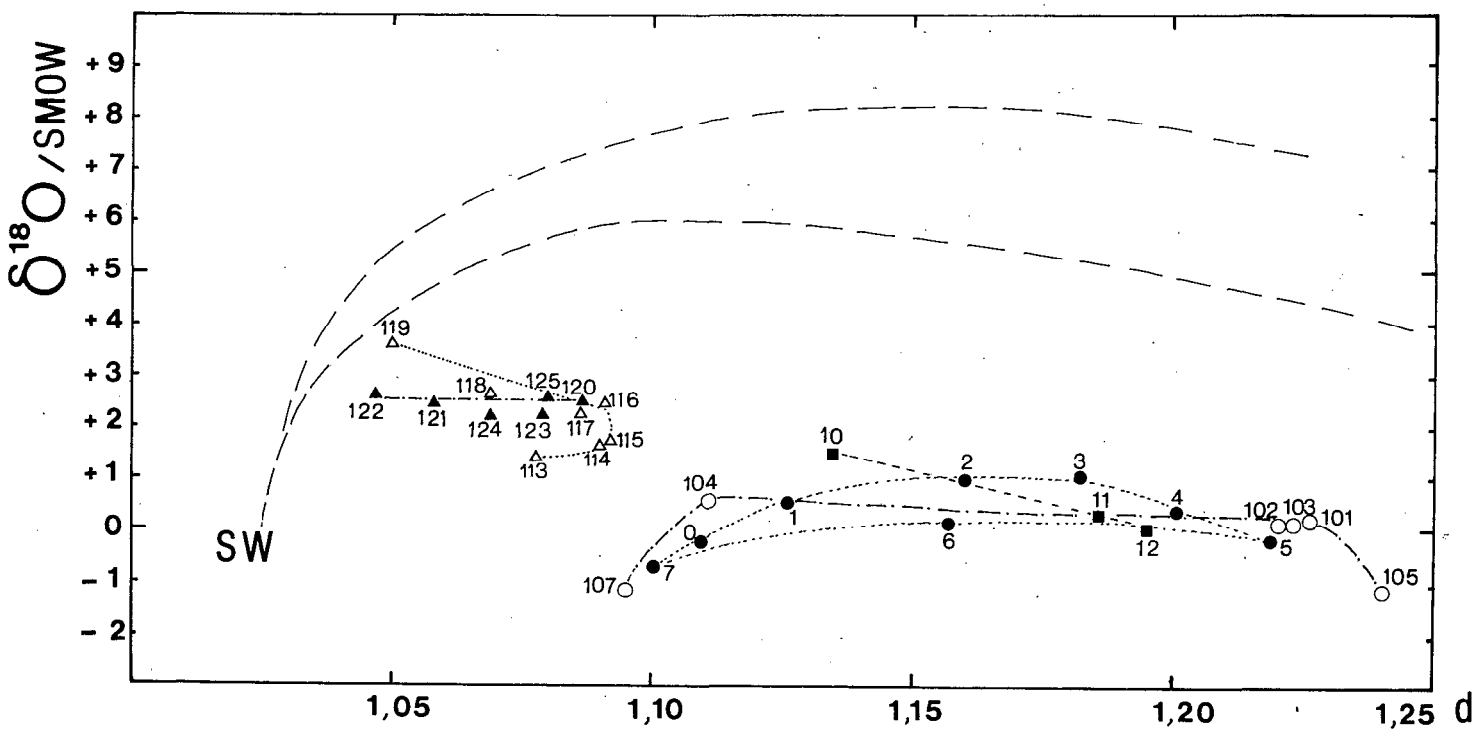

Figure 20. OXYGEN ISOTOPE COMPOSITIONS OF INTERSTITIAL SOLUTIONS (RELATIVE TO DENSITIES) FROM ALL THE STUDIED SAMPLES IN THE SOUTHERN PART OF THE OJO DE LIEBRE COMPLEX; EVOLUTION OF SEA WATER BODY DURING EVAPORATION IS GIVEN BY COMPARISON.

Table 6 = Physico-chemical, chemical and isotopic data of interstitial solutions from the salt-pan of the southernmost part of Ojo de Liebre complex

	density	pH	Eh (mV)	t°C	Na^+ m/kg	Cl^- m/kg	K^+ 10^{-3}m/kg	Mg^{2+} 10^{-3}m/kg	Ca^{2+} 10^{-3}m/kg	SO_4^{2-} 10^{-3}m/kg	T.A.C. $CaCO_3$mg/l	$\delta^{18}O$/SMOW (H_2O)
L 10	1.136	6.80	+460	22.5	3.53	3.87	46.7	227.4	44.1	78.1	40	+1.30
L 11	1.186	6.55	+440	23	4.94	5.54	61.5	265.7	54.2	50.3	31	-0.05
L 12	1.195	6.30	+200	22	5.40	6.09	65.7	243.5	78.6	30.6	33	-0.20

Table 7 = Chemical and isotopic compositions of dolomites from the salt-pan in the southernmost part of Ojo de Liebre complex

	Mole % $MgCO_3$	$\delta^{18}O$/P.D.B.	$\delta^{13}C$/ P.D.B.
L 10	45	+4.61 (+3.81*)	-4.40
L 11	45.5	+4.20 (+3.40*)	-3.71
L 12	46	+3.82 (+3.02*)	-5 27

* ^{18}O values corrected for the isotopic fractionation during the H_3PO_4 reaction (Sharma and Clayton 65)

MINERALOGY AND GEOCHEMISTRY OF SABKA SEDIMENTS AND BRINES: SECTIONS C_1 & C_2 (C.P., L.O.)

Sedimentary deposits

(See Figs. 9, 21, 22 and 23)

After the first discovery of polyhalite ($K_2MgCa_2(SO_4)_4\ 2H_2O$) by Holser (1966), and when the supratidal areas of Ojo de Liebre complex already had been transformed for the brines concentration, more occurrences of this evaporitic mineral were searched for, peculiarly along the eastern and southeastern margins of the Ojo de Liebre complex. Polyhalite was finally found in the southeastern part of the complex, in a salt pond recently isolated from the evaporitic flats by a new dike. The section C_1, across the basin, was studied in 1979 and 1980. The section C_2, oriented along the main axis of the pond and ending near the dike, was studied in 1980. Location of these two sections is given in Fig. 9. Descriptions of the geological setting and of some sedimentological aspects of this area will be published promptly (Ortlieb and Pierre, in preparation).

In section C_1, the evaporite sediments are mainly represented by gypsum with a maximal thickness of 30 cm in the centre of the basin (Fig.21). The gypsum crystals have a lenticular habit which indicates that they have grown displacively in the host detrital sediment (Shearman, 1971); they become larger (up to 1 cm) at depth and may form hard concretions (Pierre and Ortlieb, in press). In may 1979, polyhalite was only present, as small white nodules, at a few centimetres below the surface and about 10 cm above the water table. The formation of polyhalite obviously resulted from the diagenetic alteration of former gypsum (which may be observed in the core of some nodules).

In may 1980, the evaporitic sequence was strongly modified, since the lowest gypsum layers were completely replaced by a few centimetres thick polyhalite layer, somewhat indurated (Fig.22). The polyhalite was lying just below the water table, the level of which was slightly lower than a year before. These observations argue for the diagenetic replacement of gypsum by polyhalite; this replacement appears to be a very rapid process due to variations in brine chemistry (Pierre, 1981).

In section C_2 at the northwestern margin of the studied basin where solutions are seeping from the adjacent basin, a hard layer (more than 10 cm thick) of halite associated with gypsum was found at a 15 cm depth (Fig.22). Halite and gypsum crystals are large (up to 1 cm) and entirely invaded by sand grains; this argues for the diagenetic emplacement of both halite and gypsum in the sandy host sediment. Gypsum crystals may form clusters, and appear as the first diagenetic generation since some gypsum crystals are included in halite crystals.

Interstitial solutions: physico-chemical data

(See Figs. 13 to 19 and Table 8)

Brine densities are increasing and pH values are decreasing (due to decreasing water activities) from the edge towards the centre of the pond. Very high redox potential values indicate that environmental conditions are oxidizing.

Ionic concentrations of solutions collected in 1979 were not representative of normal marine derived brines. The main variations were related to higher (SO_4^{2-}) and lower (Ca^{2+}) concentrations, and to low total alcalinities. These data may be interpreted as the result of gypsum dissolution, and of a possible $CaCO_3$ crystallization.

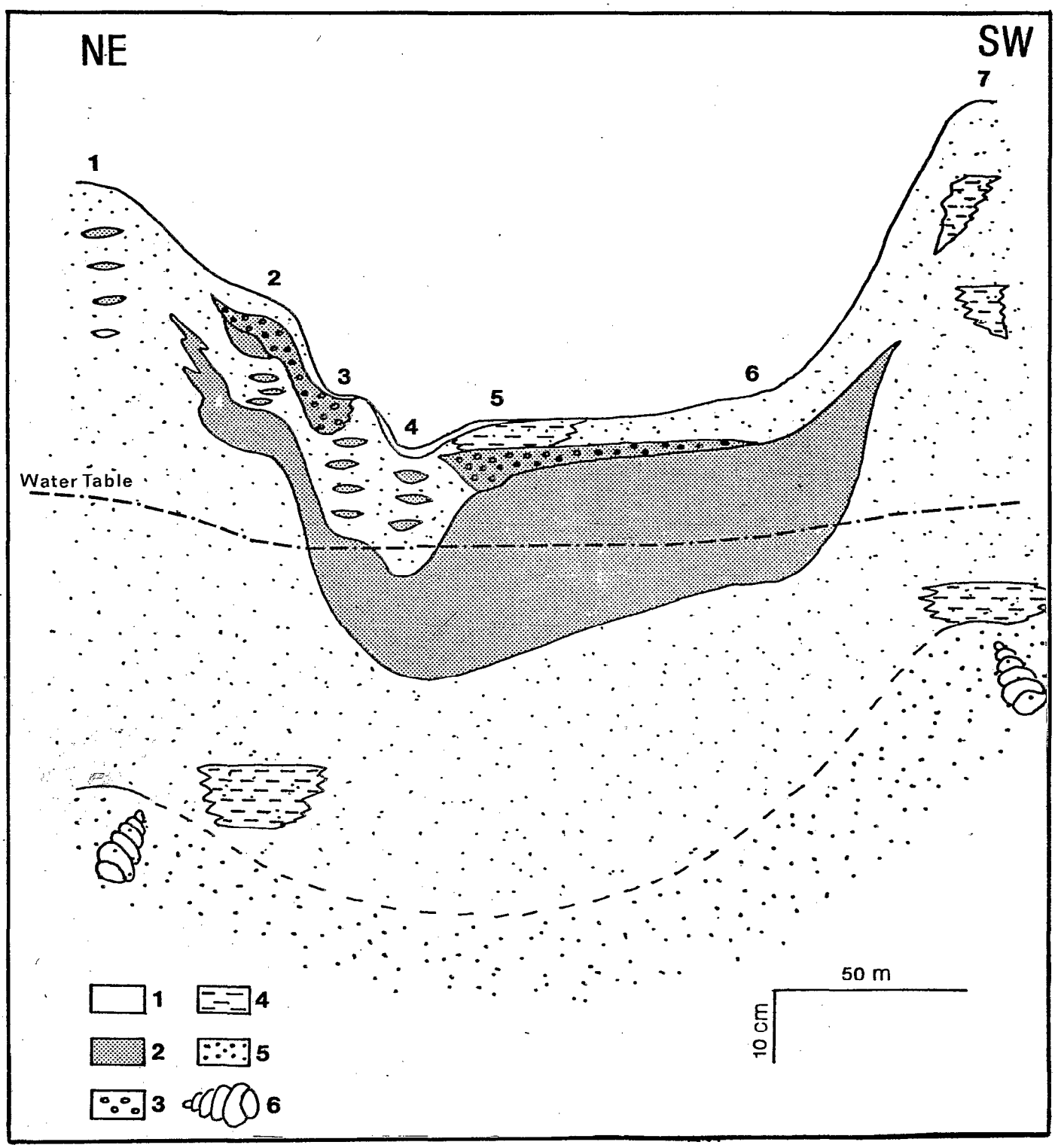

Figure 21. Cross-section C_1 of a salt pond located in the southeastern part of Ojo de Liebre complex (in may 1979): samples 1 to 7 (localization Fig. 9). Legend: 1: halite; 2: gypsum; 3: polyhalite; 4: clay; 5: sand; 6 : marine shells.

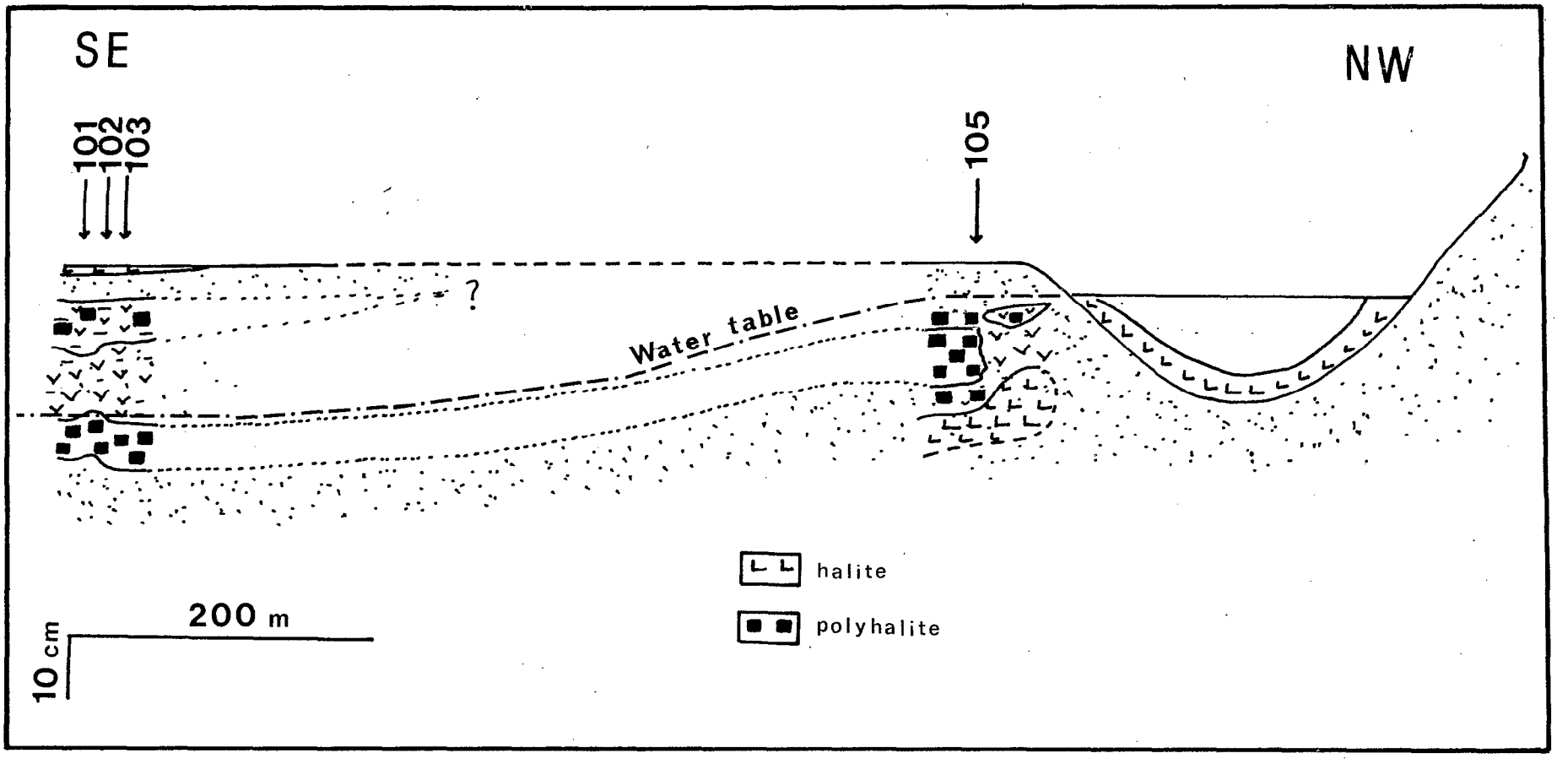

Figure 22. CROSS-SECTION C_2 IN THE NORTHWESTERN END OF A SALT POND IN THE SOUTHEASTERN PART OF OJO DE LIEBRE COMPLEX (IN MAY 1980): SAMPLES 101 TO 105 (LOCALIZATION FIG. 9).

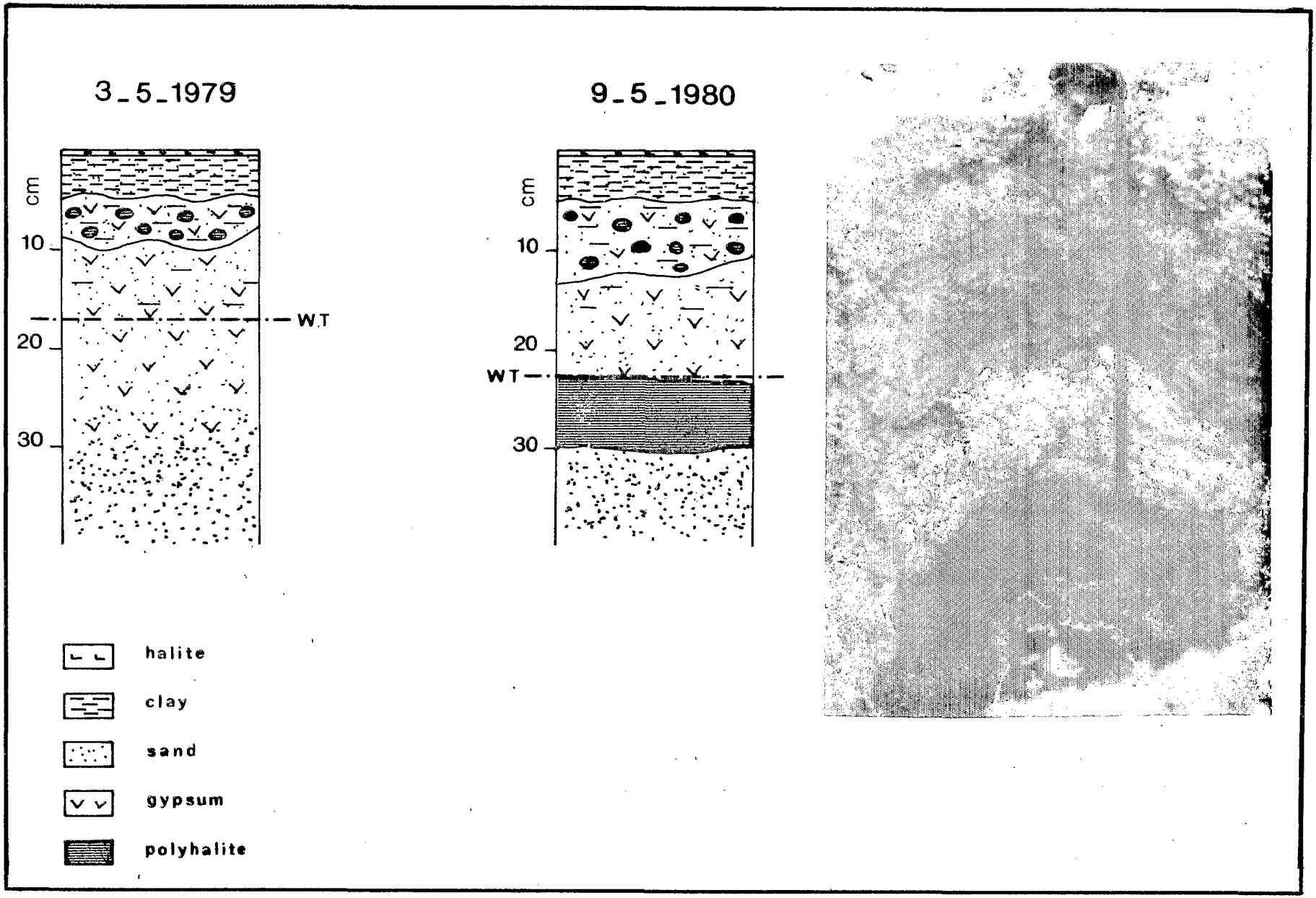

Figure 23. EVOLUTION BETWEEN MAY 1979 AND MAY 1980 OF A SEDIMENTARY SEQUENCE, IN THE CENTRE OF THE STUDIED SALT POND IN THE SOUTHEASTERN PART OF OJO DE LIEBRE COMPLEX.

Table 8 = Physico-chemical, chemical and isotopic data on interstitial solutions from supratidal areas in the southeastern part of Ojo de Liebre complex

	density	pH	Eh (mV)	t°C	Na^+ m/kg	Cl^- m/kg	K^+ 10^{-3}m/kg	Mg^{2+} 10^{-3}m/kg	Ca^{2+} 10^{-3}m/kg	SO_4^{2-} 10^{-3}m/kg	T.A.C. $CaCO_3$ Mg/l	$\delta^{18}O/SMOW$ (H_2O)	$\delta^{18}O/SMOW$ (SO_4)	$\delta^{34}S/C.D.$ (SO_4)
L 0	1.110	not measured			2.79	2.39	17.4	47.6	16.8	231.6	135	-0.2	+11.3	+18.5
L 1	1.126	7.45	+210	23.5	3,24	2.84	27.7	51.5	16.3	275.8	122	+0.5	+10.2	+18.1
L 2	1.160	7.30	+370	25	4.18	3,62	34.6	65.5	13.0	347.8	95	+0.9	+10.1	+17.3
L 3	1.182	7.15	+360	26	4.83	4,32	38.1	73.7	11.0	385.5	92	+0.9	+10.5	+18.3
L 4	1.200	6.75	+370	26	4.74	5.13	157.2	577.4	9.4	416.4	100	-0.4	+ 9.5	+18.1
L 5	1.218	6.15	+410	25.5	4.59	5.66	244.6	873.6	8.0	512.5	78	-0.1	+10	+19.0
L 6	1.157	7.10	+330	26.5	4.02	3.68	56.1	169.0	13.7	343.6	102	+0.1	+ 9.5	+17.8
L 7	1.100	7.15	+390	23	2.39	2,24	36.6	106.6	22.4	191.1	112	-0.7	+ 9.7	+17.4
L 101	1.226	6.40	+340	23								+0.2		
L 102	1.220	6.50	+285	23.5								+0.1		
L 103	1.223	5.55	+280	23								+0.1		
L 104	1.111	8.00	+340	23								+0.6		
L 105	1.240	6.30	+400	24								-1.1		
L 107	1.095	7.80	+390	24								-1.2		

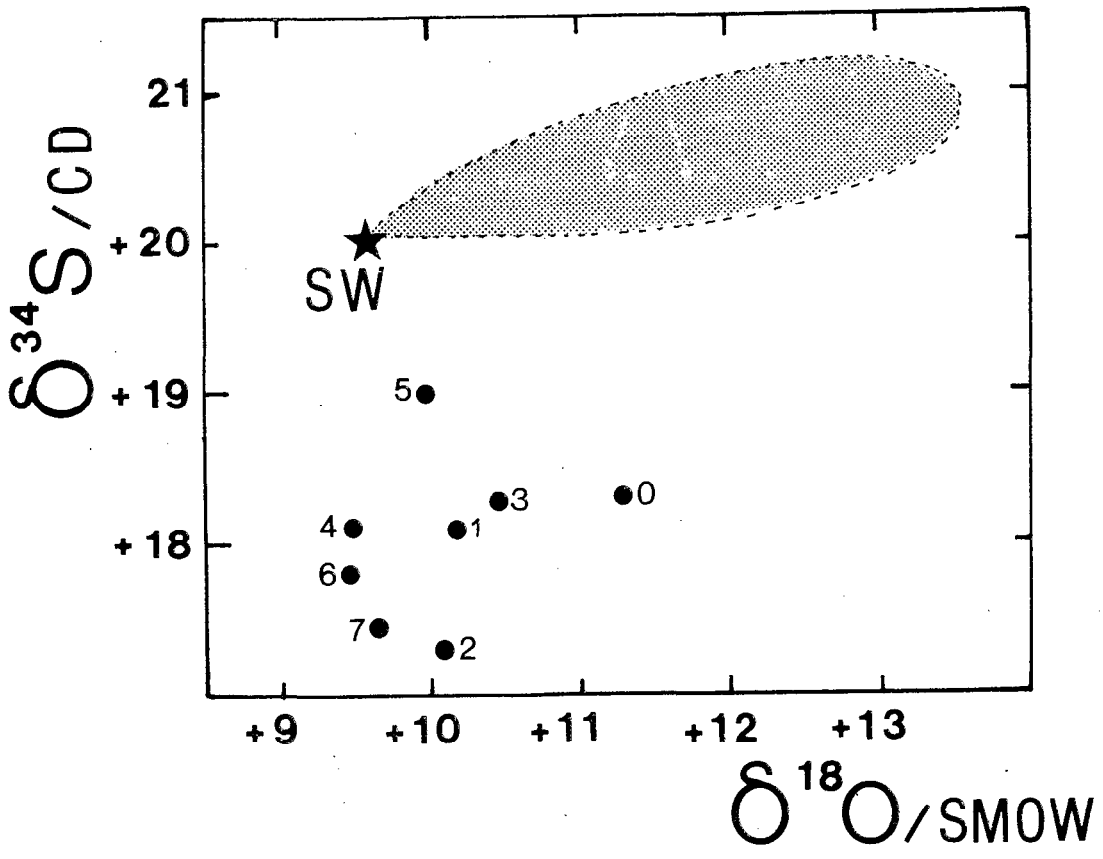

Figure 24. Oxygen and sulphur isotope contents in aqueous sulphate of interstitial solutions from the southeastern supratidal flat. The shaded area represents values observed in salt ponds from the south of France (Fontes & Pierre, 1978; Pierre, unpublished).

Stable isotopes geochemistry

(See Figs. 20 and 24 and Table 8)

The heavy isotopes contents were measured for ^{18}O in waters (collected both in 1979 and 1980), and for ^{18}O and ^{34}S in dissolved sulphate from waters collected in 1979.

$\delta^{18}O$ values of interstitial brines collected in 1979 and in 1980 are quite similar; they have a small range of variations ($-1,2\ ‰ < \delta^{18}O < +1,0\ ‰$) and do not correspond to evaporated marine waters. It appears that a large fraction of meteoric water is responsible for the negative $\delta^{18}O$ values. It hence follows that solutions are resulting from a mixing of marine brines (seeping from the adjacent basin) and of continental waters (Pierre and Ortlieb, in press).

$\delta^{18}O$ and $\delta^{34}S$ contents in dissolved sulphate have a wide range of variations ($+9,5\ ‰ < \delta^{18}O < +11,3\ ‰$; $+17,3\ ‰ < \delta^{34}S < +19,0\ ‰$). These values are far from those of the sea water sulphate ($\delta^{18}O = +9,5\ ‰$; $\delta^{34}S = +20\ ‰$). Since oxidizing conditions preclude any bacterial sulphate reduction in this basin, the δ values are interpreted as resulting from the mixing of two different sulphate reservoirs. One fraction of sulphate might be provided by marine brines while the other part might come from the dissolution of gypsum by continental waters.

Conclusions

The sulphate diagenesis is expressed in the evaporite deposits of supratidal flats from the southeastern part of the Ojo de Liebre complex by crystallization and dissolution of gypsum and by the replacement of gypsum by polyhalite. Isotopic data show that interstitial solutions are a mixing of marine derived brines and of continental waters. Aqueous sulphate has a double origin; one part is marine derived; the other part comes from the dissolution of sulphate minerals by continental waters. It is probable that in this basin, both high contents in magnesium and potassium in marine brines, as well as large inputs of sulphate ions (by gypsum dissolution) are enhancing the formation of polyhalite.

REFERENCES

Claypool, G.E., Holser, W.T., Kaplan, I.R., Sakai, H., and Zak, I., 1980, The age curves of sulfur and oxygen isotopes in marine sulfate and their mutual interpretation: Chemical Geology, v. 28, p. 199-260.

Clayton, R.N., and Epstein, S., 1958, The relationship between $^{18}O/^{16}O$ ratios in coexisting quartz, carbonate and iron oxides from various geological deposits: Journal of Geology, v. 66, p. 352-373.

Clayton, R.N., Jones, B.F., and Berner, R.A., 1968, Isotope studies of dolomite formation under sedimentary conditions: Geochimica et Cosmochimica Acta, v. 32, p. 415-432.

Engel, A.E.J., Clayton, R.N., and Epstein, S., 1958, Variation in the isotopic compositions of oxygen in the Leadville limestone (Mississipian Colorado) and in its hydrothermal and metamorphic phases: Journal of Geology, v. 6, p. 374-393.

Fontes, J.C., Fritz, P., Gauthier, J., and Kulbicki, G., 1967, Minéraux argileux, éléments traces et compositions isotopiques($^{18}O/^{16}O$ et $^{13}C/^{12}C$) dans les formations gypsifères de l'Eocène superieur et de l'Oligocène de Cormeilles-en-Parisis: Bulletin du Centre de Recherche de Pau., Société Nationale des Petroles d'Aquitaine, p. 315-366.

Fontes, J.C., Kulbicki, G., and Letolle, R., 1969, Les sondages de l'atoll de Mururoa: apercu géochimique et isotopique de la série carbonatée: Cahiers du Pacifique, v. 13, p. 69-74.

Fontes, J.C., Fritz, P., and Letolle R., 1970, Composition isotopique, mineralogique et genèse des dolomies du Bassin de Paris: Geochimica et Cosmochimica Acta, v. 34, n°3, p. 279-294.

Fontes, J.C., and Perthuisot, J.P., 1971, Facies minéralogiques et isotopiques des carbonates de la sebkha el Melah (Zarzis, Tunisie). Les variations du niveau de la Méditerranée orientale depuis 40 000 ans: Revue de Géographie Physique et de Géologie Dynamique, (2), v. XIII, fasc. 4, p. 299-314.

Fontes, J.C. and Pierre, C., 1978, Oxygen 18 changes in dissolved sulphate during sea water evaporation in saline ponds: Tenth International Congress on Sedimentology, Jerusalem, Abstr. vol., p. 215-216.

Fritz, P., and Smith, D.G.W., 1970, The isotopic composition of secondary dolomites: Geochimica et Cosmochimica Acta, v. 34, p. 1161-1173.

Gardner, E.S., 1963, Hunting the desert whale: Jarrolds, London, 256 p.

Gat, J.R., 1980, Isotope hydrology of very saline lakes, in Nissenbaum, A. (ed.), Hypersaline brines and evaporitic environments, Amsterdam, Elsevier Scientific Publishing Company, p. 1-7.

Goldsmith, J.R., and Graf, D.L., 1958, Relations between lattice constants and composition of the Ca-Mg carbonates: American Mineralogist, v. 43, p. 84-101.

Gonfiantini, R., 1965, Effeti isotopi nell'evaporazione di acque salate: Atti della Societa Toscana cli Scienze Naturali, Ser. A., v. 72, p. 1-22.

Graf, D. L., Eardley, A. J., and Shimp, N. F. 1961, A preliminary report on magnesium carbonate formation in glacial Lake Bonneville: Journal of Geology, v. 69, p. 219-223.

Guinn, J. M., 1909, Las salinas (the salt pits) : Historical Society of Southern California Publications, v. 7, p. 169-175.

Hastings, R. J. R., and Turner, R. M., 1965, Seasonal precipitation regimes in Baja California, Mexico: Geografiska Anneler, v. 47A, p. 204-223.

Hermann, A. C., and Knake, Doris, 1973, Geochemistry of modern seawater and brines from salt pans: Main components and bromine distribution: Contributions to Mineralogy and Petrology, v. 40, p. 1-24.

Holser, W. T., 1966, Diagenetic polyhalite in recent salt from Baja California: American Mineralogist, v. 51, p. 99-109.

Holser, W. T., 1979a, Mineralogy of evaporites: Mineralogical Society of America Review in Mineralogy, v. 6, p. 211-294.

Holser W. T., 1979, Trace elements and isotopes in evaporites: Mineralogical Society of America Reviews of Mineralogy, v. 6, p. 295-346.

Holser, W. T., and Kaplan, I. R., 1966, Isotope geochemistry of sedimentary sulfates: Chemical Geology, v. 1, p. 93-135.

Horosyski, R. J., and Vonder Haar, S. P., 1975, Recent calcareous stromatolites from Laguna Mormona (Baja California) Mexico: Journal of Sedimentary Petrology, v. 45, p. 894-906.

Javor, B. J., 1977, $CACO_3$ precipitation from hypersaline seawater, a working model (Abstr.): Geological Society of America Abstracts with Programs, v. 9, p. 1036.

Javor , B. J., 1979, Ecology, physiology, and carbonate chemistry of blue-green algal mats, Laguna Guerrero Negro, Mexico (PhD Thesis): Eugene, Oregon, Univ. Oregon.

Kinsman, D. J. J., 1967, Huntite from a carbonate- evaporite environment: American Mineralogist, v. 52, p. 1332-1340.

Kinsman, D. J. J., 1969, Modes of formation, sedimentary associations and diagnostic features of shallow water and supratidal evaporites: American Association of Petroleum Geologists Bulletin, v. 53, no. 4, p. 830-840.

Kirkland, D. W., Bradbury, J. P., and Dean, W. E. , Jr.,1966, Origin of Carmen Island salt deposit, Baja California, Mexico: Journal of Geology, v. 74, p. 932-938.

Larsen, H.. 1980, Ecology of hypersaline environments: in Nissenbaum, A. (ed.) Hypersaline brines and evaporitic environments, Amsterdam, Elsevier Scientific Publishing Company, p. 23-39.

Matthews, A., and Katz, A., 1977, Oxygen isotope fractionation during the dolomitization of calcium carbonate: Geochimica et Cosmochimica Acta, v. 41, p. 1431-1438.

Mina, U. F., 1957, Bosquejo geológico del territorio sur de la Baja California: Asociación Mexicana de Geólogos Petroleros, Boletín, v. 9, p. 139-269.

Ortlieb, L., and Pierre, C., (in prep.) Genesis evaporítica en tres areas supralitorales de Baja California; contextos sedimentarios y procesos actuales.

Philp, R.P., Brown, S., Calvin, M., Brassell, S., and Eglinton, G., 1975, Hydrocarbon and fatty acid distributions in recently deposited algal mats at Laguna Guerrero, Baja California: in, Krumbein, W.E. (ed.) Environmental biogeochemistry and geomicrobiology, Ann Arbor, MI, Ann Arbor Scientific Publishing, Inc., v. 1, p. 255.

Phleger, F.P., 1965, Sedimentology of Guerrero Negro Lagoon, Baja California, Mexico: Colston Papers, v. 17, p. 205-237.

Phleger, F.B., 1969, A modern evaporite deposit in Mexico: American Association of Petroleum Geologists Bulletin, v. 53, p. 824-829.

Phleger, F.B., and Ewing, G.C., 1962, Sedimentology and oceanography of coastal lagoons in Baja California, Mexico: Geological Society of America Bulletin, v. 73, p. 145-182.

Pierre, C., 1981, Polyhalite transformation after gypsum during a period of one year at Ojo de Liebre Lagoon (Baja California, Mexico). Mineralogical, chemical and isotopic evolution in sediments and associated brines (abstr.) : Geological Society of America Abstracts with Programs, v. 12, (in press).

Pierre, C., and Fontes, J.C. 1979, Oxygen 18, carbone 13, deutérium et soufre 34: marqueurs géochimiques de la diagenèse et du paléomilieu évaporitiques du Messinien de la Méditerranée: Bulletin Museum National d'Histoire Naturelle, Paris, 4^{e} Ser.,v. 1, sect. C., n°1, p. 3-18.

Pierre, C., and Person, A., 1981, Early magnesian diagenesis in carbonate sediments from supratidal evaporite flats in Ojo de Liebre Lagoon (Baja California) Mexico: (abstr.): Geological Society of America Abstracts with Programs, v. 12, (in press).

Pierre, C., and Ortlieb, L., in press, Sédimentation et diagenese dans trois lagunes évaporitiques de Basse Californie (Mexique). Données géochimiques et isotopiques sur les évaporites et les saumures interstitielles: Sciences de la Terre, (in press).

Scammon, C.M., 1869, Report of Captain C.M. Scammon, of the U.S. Revenue Service, on the west coast of Lower California: in Browne, J.R., Resources of the Pacific Slope, New York, D. Appleton and Co., p. 123-125.

Scammon, C.M., 1969, The marine mammals of the north-western coast of North America and the American whale fishery: Riverside, CA, Manessier Publishing Co. (facsimile of 1874 edition, with an introduction).

Scammon, C.M., 1970, Journal aboard the Bark Ocean Bird on a whaling voyage to Scammon's Lagoon, Winter of 1858-1859 (D.A. Henderson, ed.) : Los Angeles, Dawson's Book Shop, 78 p.

Sharma, T., and Clayton, R.N., 1965, Measurement of $^{18}O/^{16}O$ ratios of total oxygen of carbonates: Geochimica et Cosmochimica Acta. v. 29. p. 1347-1353.

Shearman, D. J., 1970, Recent halite rock, Baja California, Mexico: Transactions of the Institution of Mining and Metallurgy, Sec. b, v. 79, p. 155-162.

Shearman, D. J., 1971, Marine evaporites; the calcium sulphate facies:(Unpublished report), The University of Calgary, A. S. P. G. Seminar, 65 p.

Smith, S. M. B., 1973, Halite crystallization in supratidal salina, Ometepec Lagoon, Baja California, Mexico(abstr.): American Association of Petroleum Geologists Bulletin, v. 57, p. 805.

Vonder Haar, S. P., 1975, Evaporites and algal mats at Laguna Mormona, Pacific Coast, Baja California, Mexico (Ph. D. thesis) : Los Angeles, University of Southern California.

Vonder Haar, S. P., and Gorsline, D. S., 1975, Flooding frequency of hypersaline coastal environments determined by orbital imagery: Geologic implications: Science, v. 190, p. 147-149.

Vonder Haar, S. P., and Gorsline, D. S., 1977, Hypersaline lagoon deposits and processes in Baja California, Mexico: Geoscience and Man, v. 18, p. 165-177.

Wittich, E., 1916, Die Salzlager an Ojo de Liebre an Westkuste Von Nieder-Kalifornien. Centralblatt für Mineralogie, Geologie und Paläontologie, 1916, p. 25-32.

Zarate, J. C., 1917, Las salinas de Mexico y la industria de la sal común: Anales del Instituto Geológico de México, v. 2, 71 p.

GEOCHEMISTRY AND ECOLOGY OF SALT PANS AT GUERRERO NEGRO, BAJA, CALIFORNIA

ROAD LOG

km (mi)	
0 (0)	Leave gates through the salt company facilities at Guerrero Negro. The first several miles lead through NaCl crystallizing ponds followed by low, stabilized dunes of quartz sands, shells, and detritus from an earlier lagoon cycle. Sea water concentrating ponds (gypsum stage) are visible in the distance on the left (east).
23.8 (14.9)	Road junction. At the right is the turn-off to the whale-watching park. Straight ahead are low dunes, blue-green algal flats (Lyngbya aestuarii and Calothrix crustacea), salt marshes,
STOP 1	and Laguna Ojo de Liebre. To the left is sea water concentrator Area 9 which is characterized by a floor of gypsum. Note the difference in the crystal habits on the undersides (subaqueous) and surfaces of the gypsum crusts, as well as the "teepee" structures. The underside of the crust is colonized by blue-green algae (coccoid, Aphanothece halophytica), below which are purple photosynthetic bacteria. Ephydra fly pupal cases are common.
24.8 (15.5)	Follow the road east past the former seawater pumping station.
25.0 (15.6)	Turn left on dike 9 just before arriving at a former pumping station. On the left is concentrator 9 (annual range of density 1.103-1.133). On the right is concentrator 8 (annual
STOP 2	range of density 1.094-1.111). Concentrator 8 is characterized by a soft algal mat floor at the entrance (largely coccoid blue-green algae and diatoms), with gradually more and more sand-size crystals of gypsum at the base of the photosynthetic zone (about 1 cm below the mat surface) in the higher salinity areas of the pond. Cores of the mat (several cm thick) demonstrate that gypsum also precipitates at the base of the older photosynthetic layers. Area 9 is characterized by algal and gypsum-sand mats at the entrance but most of this concentrator is covered with a firm gypsum crust. The algal mat covers the surface of the crust at lower salinities and eventually only the undersides of the crust at higher salinities. Note the "hummocky" nature of the gypsum crust in Area 9 along the dike (lithified ripples).
28.5 (17.8)	Junction of dikes 8 and 9 (Areas 6, 8, and 9). Turn right. Concentrator 6 (annual range of density 1.066-1.090) is characterized by the same mat as in 8, but gypsum precipitation does not occur at the lower densities in this pond. The orange color of the algae is caused by the predominance of carotenoid pigments.
29.3 (18.3)	Junction of dikes 7 and 8 (concentrators 6, 7, and 8). Concentrator 7 was filled in Winter, 1979, but fauna, flora, and sediments have not yet stabilized.

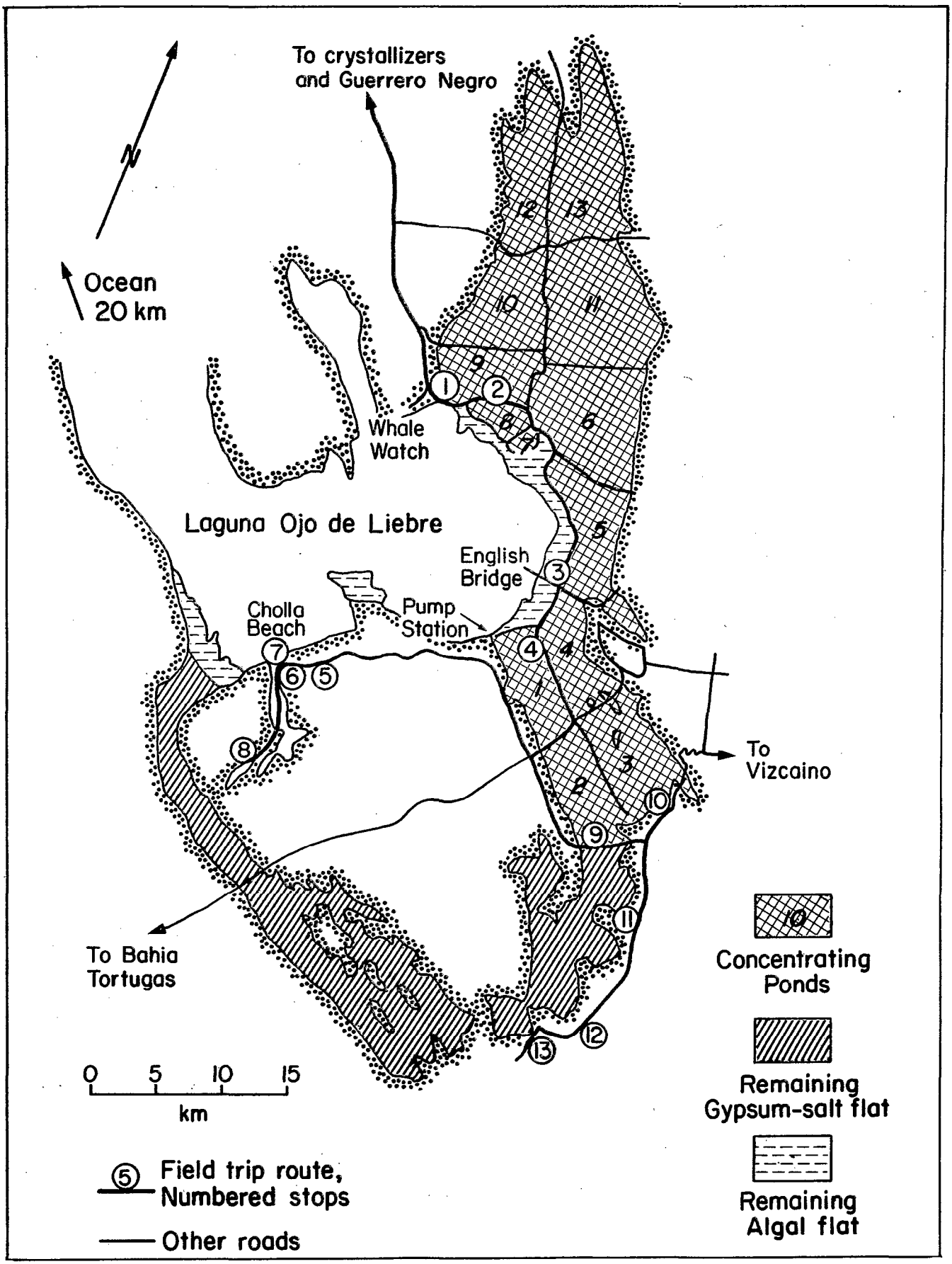
To crystallizers
and Guerrero Negro
Ocean
20 km
Whale
Watch
Laguna Ojo de Liebre
English
Bridge
Cholla
Beach
Pump
Station
To
Vizcaino
To Bahia
Tortugas
0 5 10 15
km
Field trip route,
Numbered stops
Other roads
Concentrating
Ponds
Remaining
Gypsum-salt flat
Remaining
Algal flat

30.1 (18.8) — Former pumping channel. This is the beginning of the route characterized by natural salt marshes and algal flats on the right (west) which are truncated by the dike and sea water concentrators on the left. This area corresponds to the toe of the boot-shaped Laguna Ojo de Liebre.

31.4 (19.6) — Corner of Areas 5 and 6. Continue to the right.

33.0 (20.6) — "Patch" in dike where old gypsum floor was broken during construction. Because so much brine leaked out from the pond, a new retaining wall was built using the nearly impermeable gypsum crust as the floor. Concentrator 5 algal mats are dominated by filamentous blue-green algae (largely Microcoleus chthonoplastes). Diatoms and photosynthetic bacteria also occur (annual range of density 1.047-1.070).

(possible additional stop)

34.7 (21.7) — Note the presence of large dark clumps in the dike wall. These are old algal mats excavated during dike construction.

37.0 (23.1) — Note the old pilings from a former salt-loading railroad on the right. Note that the Salicornia-dominated salt marshes have given way to blue-green algal flats as we move further leeward on the lagoon shoreline. The associated sediments include more aragonite and less siliceous sand further landward from the lagoon. Some recrystallization to dolomite may be occurring within the sediment (results from X-ray diffraction analyses).

39.0 (24.4) — Former pumping station.

41.0 (25.6) — "English Bridge" on the right (a former salt-loading facility). Cores through the sediments here show alternating layers of dead sea grass (Zostera), blue-green algal mats, quartz sand, gypsum, carbonates, and clay. Note the association of lensoid gypsum crystals (sand to cm size, not cemented) with algal layers. Also note the lensoid gypsum crystals in the dike walls. This locality is not accessible during or following high tides. If not, continue to mile 27.7. Section A (Figs. 2-8), sampled by Holser before construction of the concentrators, started where the "Bridge" crosses the shore, intersected the route of the field trip at this stop, and continued to the landward end of the small salina to the east.

STOP 3

42.4 (26.5) — Concentrator 4 on the left. Large (up to several decimeters), laminated (stromatolitic but not lithified) blocks occur near the edge of the concentrator (annual range of density 1.036-1.066). The species are basically the same as those in Area 5. Due to competition by other algae and grazing by fish and invertebrates, algal mats (stromatolites) do not occur in the ponds of lower concentration.

(possible additional stop)

44.3 (27.7) About 100-200 m before the gate to pump station 3A, a finger of the lagoon reaches the road. Within a short walking distance, middle intertidal blue-green algal mats (Lyngbya aestuarii) grade into upper intertidal Calothrix crustacea mats, above which are evaporite flats. Sections through these sediments show stratigraphy similar to those at the English Bridge (mile 25.6). However, at this locality a rather impermeable layer of coquina lies at about 0.5 m depth.

44.5 (27.8) Gate to the present pumping station 3A. Turn to the left and cross the natural isalnd in the former tidal flats. Note the former beach fauna and Indian midden remains (obsidian chips, shells, bones).

44.8-46.4 (28.0-29.0) STOP 4 Sediments on the shore of the former island are covered with shells. Just below the surface is a layer of coffee-colored carbonate-siliceous sands. Between 10-20 cm below the surface is a layer of gypsum, some is nodular, like powder sugar, and white- to buff-colored. Below the gypsum is about 30 cm of light colored carbonate-siliceous sands with shells.

53.6 (33.5) Junction of concentrators 9, 2, 3, and 4 (center of former "Salina Grande"). Turn right and follow sign to Bahía Tortugas and Asunción. Holser (1966) found polyhalite also in this section of the original sabkha (Fig. 2, Section B).

56.5 (35.3) At the end of the dike is a 3-way junction. Turn right and follow the road closest to the shore of the evaporator.

64.8 (40.5) Gate to the pump station. Turn left and follow the road closest to the lagoon.

66.6 (41.6) Junction to a fisherman's camp on the shore at the right. Take the left and continue following the shore of the lagoon. The track may be very poor in places.

74.2 (46.4) STOP 5 This marks the beginning of a very long (several km), high intertidal-supratidal flat. Sediment cores in this area have a mixture of gypsum, carbonate, and siliceous sand. A gypsum layer is especially noticeable below buried layers of sea grass. Pierre and Ortlieb found dolomite in this area (Fig. 2, Section E).

77.1 (48.2) STOP 6 Just before the fisherman's camp at Cholla Beach. The surface carbonate muds are immediately underlain by gypsum. Abruptly at ca. 20 cm depth is a rust-colored layer of lensoid gypsum crystals (about 2 mm diameter crystals). This layer is about 20 cm thick and is underlaid by carbonate sediments of the same color.

77.8 (48.6) STOP 7 — Cholla Beach. Shore sediments are siliceous and carbonate sands and muds with gigantic windrows of sea grass washed in from the lagoon. Note the windrows of foraminifera on the beach below the sea grass.

80.5 (50.3) — Continue following the track inland and across the flats. Do not leave the track. A large natural salt flat can be seen on the left (east).

81.1 (50.7) STOP 8 — Junction with another track and a broken road sign to Guerrero Negro. In front is a large natural salt flat. The salt is underlain only by coffee-colored carbonate-siliceous sand and occasional gypsum lenses.

105.8 (66.1) — Return to junction at 56.5 km. At the junction, continue straight (southeast) along the shore of concentrator 2.

110.2 (68.9) — Cross the canal. The canal was to be used to flood another salt flat.

112.2 (70.1) STOP 9 — Intersection with a dike. Turn left and follow the dike.

115.2 (72.0) STOP 10 — End of the dike. At this point follow left to locate the site of Pierre and Ortlieb's sampling locality, on a part of the sabkha separated from concentrator 3 by a short dike (Fig. 2, Section C). Return to intersection and continue south (distance not logged).

115.5 (72.2) — Crossroad (look for marker stakes). Turn right and follow the track at the edge of the salt flats 12.8 km (8.0 mi).

120.3 (73.4) STOP 11 — Most of this extensive salt flat is covered by gypsum sand with some quartz and carbonate sand abruptly underlain at about 10 cm depth by sand-size, lensoid crystals of gypsum. At about 30 cm depth blocky gypsum begins. In some places below the blocky gypsum lies a layer of siliceous-carbonate sand (ca. 10 cm) which is again underlain by gypsum. Some of the blocky gypsum, which is generally a dusky color, contains "cores" (small local seams) of uncemented, white, sand-size crystals.

123.7 (77.3) — The road climbs about 3 or 4 meters on a low dune. Just ahead the road branches. Keep to the right, staying near the salt flat.

124.3 (77.7) (possible additional stop)
The road returns to the edge of the salt flat. Notice the sediment here is covered with pebbles (predominantly basalt). Sediment cores yield a mixed gypsum-carbonate mud. At about 50 cm lies a fairly impermeable carbonate layer. Within the top 50 cm are occasional rounded cobbles of diverse lithologies.

126.2 (78.9) STOP 12
Large gypsum roses occur in the road cut. They appear to be recrystallization products of the large, blocky gypsum crystals that outcrop here. Note the erratic basalt boulders on the salina floor. Halite occurs only as a thin veneer. These are the furthest inland salt flats of the Laguna Ojo de Liebre sabkha.

128.3 (80.2) STOP 13
Continue on the track around the base of the large mesa. Note the magnesite along the road cut. At the base of the head of the mesa is an old sandstone reef similar to one found on Isla de Piedra in the lagoon. Climb the mesa for a good viewpoint. From here one can walk across the salina floor to examine more large basalt boulders. Their origin and mode of movement poses a curious geologic question. The sabkha near here was sampled by Pierre and Ortlieb (Fig. 2, Section D).

147.4 (92.1) STOP 14
Return to the canal at 110.2 km (68.9 mi). Turn left (south) 1 km (0.6 mi) up the grade following the canal. Note the sediment cross section in the canal walls as the road rises up the mesa. A viewpoint of a large salina is at the top. Sediments underlying the salt are the same as those in the salt pan near Cholla Beach.

209.3 (130.8)
Return to Guerrero Negro.